Case Studies in Thermal Engineering 64 (2024) 105560

Contents lists available at ScienceDirect

Case Studies in Thermal Engineering

journal homepage: www.elsevier.com/locate/csite

Effect of nano-particles on the combustion and emission characteristics of a dual fuel engine operated on biodiesel-producer gas combination

K.A. Sateesh [a], V.S. Yaliwal [a,***], B.K. Murugande [a], N.R. Banapurmath [b], P.V. Elumalai [m], Dhinesh Balasubramanian [c,**], Krupakaran Radhakrishnan Lawrence [d], Yasser Fouad [e], Manzoore Elahi M. Soudagar [f,g,h,i,*], Huu Cuong Le [j,****], Thanh Tuan Le [k], Md Abul Kalam [l], Chan Choon Kit [n], Yelamasetti Balram [o]

[a] Department of Mechanical Engineering, SDM College of Engineering and Technology, Dharwad, Karnataka, India
[b] Department of Mechanical Engineering, BVB College of Engineering and Technology, KLE Technological University, Hubli, Karnataka, India
[c] Department of Mechanical Engineering, Mepco Schlenk Engineering College, Sivakasi, Tamil Nadu, India
[d] Department of Mechanical Engineering, Mohan Babu University (erstwhile Sree Vidyanikethan Engineering College), Tirupati, Andhra Pradesh, India
[e] Department of Applied Mechanical Engineering, College of Applied Engineering, Muzahimiyah Branch, King Saud University, Riyadh, Saudi Arabia
[f] College of Engineering, Lishui University, Lishui, 323000, Zhejiang, China
[g] Department of Mechanical Engineering, Graphic Era (Deemed to Be University), Dehradun, Uttarakhand, 248002, India
[h] Centre of Research Impact and Outcome, Chitkara University, Rajpura, 140417, Punjab, India
[i] Division of Research and Development, Lovely Professional University, Phagwara, 44411, Punjab, India
[j] Institute of Maritime, Ho Chi Minh City University of Transport, Ho Chi Minh City, Viet Nam
[k] Institute of Engineering, HUTECH University, Ho Chi Minh City, Viet Nam
[l] School of Civil and Environmental Engineering, Faculty of Engineering and Information Technology, University of Technology Sydney, Ultimo, Sydney, NSW, 2007, Australia
[m] Department of Mechanical Engineering, Aditya University, Surampalem, 533437, India
[n] Faculty of Engineering and Quantity Survey INTI International University, Persiaran Perdana BBN, Putra Nilai, 71800, Nilai, Negeri Sembilan, Malaysia
[o] Department of Mechanical Engineering, MLR Institute of Technology, Hyderabad, Telangana, India

ARTICLE INFO

Handling Editor: Huihe Qiu

Keywords:
Dairy scum oil methyl ester
Aluminium oxide hydroxide (AlO(OH)
Producer gas
Hydrogen

ABSTRACT

In this experimental study, efforts were undertaken to augment the overall efficiency of a dual-fuel engine. This present study was conducted in three steps. In the initial phase, Aluminium oxyhydroxide (AlO(OH)) was synthesized and analyzed using UV–visible spectroscopy, XRD (X-ray diffraction), Thermogravimetric (TG) analysis, and Differential Scanning Calorimeter (DSC). In the second part of the study, the impact of AlO(OH) NP dosage on the performance of a producer gas-powered diesel engine was investigated. To optimize adequate AlO(OH) NPs

* Corresponding author. College of Engineering, Lishui University, Lishui, 323000, Zhejiang, China.
** Corresponding author.
*** Corresponding author.
**** Corresponding author.
E-mail addresses: vsyaliwal2000@rediffmail.com (V.S. Yaliwal), dhineshbala91@gmail.com, dhineshbala91@mepcoeng.ac.in (D. Balasubramanian), cuong.le@ut.edu.vn (H.C. Le).

https://doi.org/10.1016/j.csite.2024.105560
Received 20 May 2024; Received in revised form 23 November 2024; Accepted 24 November 2024
Available online 26 November 2024

Dual-fuel combustion
Emissions
Energy efficiency

addition, three working fluids are prepared by dissolving NPs in dairy scum oil methyl ester (DiSOME) biodiesel ranging from 20 to 60 ppm and varied in steps of 20. In the next phase, the present study examined the effect of 60 ppm of various NPs, including multi-walled carbon nanotubes (MWCNT), Aluminum oxide (Al2O3), and AlO(OH) on the combustion and emission characteristics of a 1-cylinder 4-stroke direct injection diesel engine operating in dual fuel mode using a combination of DiSOME and producer gas. The study concluded that DiSOME-PG operation with 60 ppm AlO(OH) and without nano-addition resulted in decreased BTE by 2.9 % and 14.6 % respectively compared to diesel-supported dual fuel operation. To the extent that exhaust levels are concerned, AlO(OH) addition to the DiSOME-PG combination lowers hydrocarbon (HC) and carbon monoxide (CO) emissions than identical fuel amalgamation without AlO(OH) NP. It is noticed that the retarded combustion related to the DiSOME-producer gas mixture can be improved with NP addition. The DiSOME-producer gas functioning with NPs addition is the individuality of this current effort.

1. Introduction

Diesel engines occupy a very significant role in shaft power applications. This is due to the fact that diesel engines are lean burn engines and provide high power output with reduced carbon-based emissions and also are more reasonably priced than counterpart petrol engines. However, these engines are prone to higher NOx and particular matter (PM) [1]. This is possible because the NOx and smoke emission formation mechanism is completely reversed compared to HC and CO formation. Hence, technology employed to reduce total emissions is difficult and not possible to meet the emission norms. To keep hold of diesel engines for greater power output, numerous researchers have tried several techniques in diesel engines using advanced technology in terms of fuel and engine design modification. Thereby better performance with reduced emissions can be observed. In this context, the use of renewable fuels is becoming increasingly important given the declining amount of subterranean underground oil, hazardous emissions, and the rising price of crude oil. Under these conditions, in the last two decades, alternative fuel derived from biomass has come out as a replacement for fossil fuels partially or completely. The use of such fuels has several benefits, i.e., they are renewable, biodegradable, and deal with social and environmental issues [2,3].

In this direction, numerous scientists have experimented with different types of biodiesels in a single fuel mode using different NPs [3–6]. Numerous researchers have reported biodiesel operation may produce a power output that is higher, lower, or equal. According to Qi et al. [7], demonstrated identical power output as that of diesel operation with lesser carbon-based emissions. When using biodiesel, combustion started earlier than when using diesel at higher loads. Furthermore, some researchers have reported lower carbon-based emissions and increased thermal efficiency in a turbo-charged diesel engine when using biodiesel fuel. This may be owing to increased amount of oxygen and cetane number, which promote more complete combustion. Nonetheless, reported elevated NOx emissions [8–10]. Contradictorily, Banapurmath et al. [11] have reported lower thermal efficiency and higher carbon-based emissions. A study has been published that examines the combustion and emission characteristics of a 4-stroke, 1-cylinder diesel engine using DiSOME [12–14]. A study revealed that, there are acceptable levels of performance and emission levels with lowered NOx, cylinder pressure, and heat release rate. In addition, Agarwal et al. [15] have investigated the effects of injection pressure, timing, and blending ratio on the performance, combustion, and emission characteristics of a common rail direct injection (CRDI) engine. According to their findings, the presence of smaller droplets improve performance and reduced CO, HC, and smoke levels when the injection timing is optimal, and the injection pressure is higher. Karthickeyan et al. [16] and Yuning et al. [17] analyzed the influence of combustion chamber geometry on the combustion and emission properties of biodiesel-fueled diesel engines. Except for NOx levels, they discovered that the toroidal combustion chamber (TCC) performed better and produced fewer emissions than the hemispherical combustion chamber (HCC). The observed trend can be attributed to amplified swirl and squish while using TCC [18]. Yuning et al. [17] developed a double swirl combustion system and reported that this provides speedy air–fuel mixing leading to greater indicated power and lower soot generation due to better motion of in-cylinder air with air entrainment. However, the main disadvantages of using biodiesel are inferior properties compared to diesel fuel. This leads to differences in spray characteristics.

Therefore, to enhance the effectiveness of diesel engines, it is essential to generate power from renewable sources through appropriate fuel modification. Therefore, several investigators have used various nano-particles (NPs) to enhance combustion efficiency and lower tail pipe emissions. This might be a result of improved thermal, and physicochemical properties [19–22]. Studies have demonstrated that raising the injection pressure and incorporating TiO2 NPs into the base fuel can enhance the combustion properties of a diesel engine [23]. Size and shape influence the functionalization of nano-particle capacity, diffusion fluid drag, and other properties. In addition, colloidal suspension stability control and its properties are advantageous in engine applications. NP enhance the air-fuel mixing, improve combustion with a decreased delay period, lowers the viscosity, and increase the energy content of base fuel [24]. A thorough examination of the use of NPs for fuel blending and their impact on combustion and emission characteristics has been conducted by Refs. [25–29]. Studies on the exergy, sustainability analysis, and performance of a diesel engine operated on a biodiesel blend with and without aluminum oxide (Al2O3) NPs have been documented and reported acceptable performance with a NP blended fuel [30–32]. In the study of Soudagar et al. [33], they found that, addition of 20 ppm Al2O3 to B20 led to a 10.57 % improvement in thermal efficiency, 11.65 % decrease in BSFC, 22 %–48.43 % decreased carbon-based emissions and 11.27 % increased NOx emissions. Further, improved combustion characteristics have been reported. Similar trends of results were documented by Refs. [31–37]. Further, diesel, biodiesel, ethanol, and carbon nano-tube blended fuel influence on the performance of a

diesel engine is examined by Ref. [38]. They found amplified power by 15.2 %, amplified thermal efficiency by 13.97 %, reduced BSFC by 11.73 %, reduced 1.86 % by EGT, reduced CO by 5.47 %–31.72 %, reduced carbon-based emissions and 12.22 % increased NO levels compared to diesel operation. The addition of 50 ppm of multi-walled carbon nanotubes in diesel-biodiesel blended fuels showed higher cylinder pressure compared to normal diesel operation [39,40]. It has also been investigated that how blended biodiesel containing calcium oxide affects the performance, emissions, and combustion characteristics of diesel engines [40]. Their statement indicates that smoke, HC, CO, and NOx emissions were reduced in comparison to diesel fuel. Furthermore, there have been reported elevated cylinder pressure and heat release rate.

Researchers have stated that dual fuel engine functioned on methanol (manifold injection)-diesel (in-cylinder direct injection) combination with cerium oxide (CeO2) nanoparticle resulted in increased heat release rate and the cylinder gas pressure compared to diesel operation. A study has shown that in dual fuel mode, there is an 8.1 % increase in BSFC, a 10.8 % increase in thermal efficiency, and reduced emissions compared to diesel mode [41,42]. Additionally, the addition of a blend of diesel and biodiesel fuel containing 60 ppm of graphene nano-platelets resulted in a 29.2 % reduction in smoke emissions and a 26.4 % reduction in NOx emissions. They observed a lower carbon-based emissions with graphene oxide addition [43]. A novel nano-particle sugarcane nano-biochar has been developed and used instead of conventional metallic-based fuel additives. Engine operation with a blend of 10 % fuel oil and 100 ppm sugarcane nano-biochar resulted in lowered NOx by 20.51 % and UHC emissions by 14.6 %, increased CO emissions by 33 % [44].

A literature study on the use of nanomaterials in biodiesel revealed improved efficiency and reduced emissions as compared to traditional biodiesel operations. But showed increased fuel consumption owing to lower energy content. However, it is noticed that dual fuel operation can reduce smoke and NOx pollutants and the lowers pilot fuel consumption. However, reduced thermal efficiency and increased emissions of HC and CO were the results of using gaseous fuel induction in a dual fuel engine [3,45–48]. Researchers suggested non-edible oils and waste-derived gaseous fuels for use in diesel engine applications. Dual fuel engines operated on non-edible oils and are used as secondary fuel and producer gas was substituted as primary fuel. Further to enhance the performance of a diesel engine, a small quantity of hydrogen can be added along with producer gas. In this context, Sahoo et al. [48], Yaliwal et al. [49] investigated the performance of dual-fuel engines operated on biodiesel-hydrogen enriched producer gas. They have reported differences in the performance caused by the involvement of gaseous fuel during combustion. Gaseous fuel does not auto-ignite under the current state of pressure and temperature circumstances. Therefore, a small amount of pilot fuel is required to start the combustion of gaseous fuel [46,47]. Research conducted on a producer gas-fueled diesel engine showed a reduction in thermal efficiency with increased carbon-based emissions, and lower NOx and smoke emissions. Furthermore, the literature reported increased ignition delay and combustion duration, decreased cylinder pressure, and rate of heat release, and resulted in 60–90 % savings on pilot fuel [4, 50–53]. Air supply circumstances, engine modifications, feedstock physical and chemical attributes, gasifier type, and other factors all had a substantial impact on overall performance and tailpipe emissions [52–56].

Effects of hydrogen addition, higher compression ratio and injection pressure, advanced injection timing, and various nozzle and combustion chamber geometries on the performance and exhaust emission levels have been stated [3,4,11,48,49,51,57–60]. Reports have indicated that advanced injection time, injection pressure of 230 bar, higher compression ratio and adequate nozzle and combustion chamber resulted in superior thermal efficiency and lower pollution levels [59]. This phenomenon may be attributed to the increased availability of time for the physical mixing of gaseous fuels with pilot fuel and the formation of smaller droplets. Increased swirl can lead to improved mixture formation and speeds up the mixing of different fuels. This is necessary to limit soot production during the expansion period and reduce specific fuel consumption [3,49,60].

2. Present work

Based on documented reports and investigator presentation, no research work has yet examined the utilization of NPs in biodiesel-producer gas-fueled diesel engine applications. This study was conducted in three stages and during the initial phase of the project, AlO(OH) was synthesized and characterized. Subsequently, in the second stage of the work, the effect of AlO(OH) NP dosage on the overall performance of a producer gas-powered diesel engine was examined and a better proportion of NP was selected. To optimize adequate AlO(OH) NPs addition, three working fluids are prepared by dissolving NPs in DiSOME biodiesel ranging from 20 to 60 ppm and varied in steps of 20. In the subsequent phase, the effects of 60 ppm concentrations of different nanoparticles, such as multi-walled carbon nanotubes (MWCNT), Aluminum oxide (Al2O3), and Aluminium oxyhydroxide (AlO(OH)), on the combustion and emission characteristics of a single cylinder four-stroke direct injection diesel engine operating in dual fuel mode with dairy scum oil methyl ester (DiSOME) - producer gas were investigated. Ultimately, the outcomes achieved using a nano-blend of biofuel has been compared with

Fig. 1. Dairy scum waste.

the standard operating mode.

3. Materials and methods

In this present work, dairy scum effluent, synthesis of AlO(OH) NPs, and biomass are discussed.

3.1. Dairy scum effluent

The scum will be accumulated from the Karnataka Milk Federation (KMF), Dharwad, Karnataka state, and obtained from the scum-eliminating part of the effluent treatment plant (Fig. 1). After that, it is treated in proper way to prevent a biological effect that would raise free fatty acid levels. Scum has a semi-solid texture and a turbid white color. A known amount of scum is heated to 100 °C to melt it into a liquid state. It is then given a few minutes to settle and the upper oil layer is separated and centrifuged.

For transesterification, dairy scum oil is heated to temperatures above 100 °C until it turns anhydrous and filtered using steel micromesh. The oil is now ready for transesterification.

3.2. Production of biodiesel and producer gas

Biomass was collected from the solid waste of municipalities (MSW). It is dried and sized about one inch and used in a down draft gasifier for producer gas generation. The primary fuel source was producer gas, which is produced using the procedure described in the literature [3,46]. Biodiesel produced from waste is being used in the current project for diesel engine applications. DiSOME is a kind of biodiesel made from dairy waste that is used in dual-fuel engines as an injected pilot or secondary fuel. For dual fuel operation, biodiesel (pilot fuel) was used as secondary fuel. Dairy scum oil methyl ester (biodiesel) was prepared according to the method outlined in the literature [14].

3.3. Properties of fuels used

The authors synthesized dairy scum oil biodiesel at a college laboratory following the specified procedures [14,61,62]. Produced gas is another combustible gaseous fuel made from municipal solid waste. Additionally, the waste biomass from MSW was utilized to generate producer gas. Biodiesel properties and proximate analysis of biomass are given in Tables 1 and 2 respectively.

4. Synthesis of AlO(OH) nano-particle

Materials used for the production of AlO(OH) nanoparticles are Aluminium nitrate (Al(NO)3), Sodium hydroxide (NaOH), and Deionized water.

Fig. 2 presents the steps involved in the synthesis of AlO(OH) nanoparticles. All solutions are prepared in ultrapure deionized water with resistance above 18 MΩ using the Millipore Milli-Q system. All chemicals of analytical grade were purchased from SD Fine Chemicals (India), India and used without further purification. A solvothermal process was used to produce the AlO(OH) nano-structures, and the nanoparticle was produced and described by existing literature [2,63]. In a typical experiment, a 1M solution of Aluminium nitrate $Al(NO)_3$ in 100 ml deionized water under a magnetic stirrer at room temperature and stayed for 30 min until metal salt completely dissolved. Then a 3M solution of sodium hydroxide NaOH of 3 M–100 ml deionized water was prepared. Further, NaOH solution is added dropwise to a solution of $[Al(NO)_3]$ by using the pipette. The transpired solution precipitated with the addition of NaOH under a magnetic stirrer. The precipitated white material is kept under stirring for 24 h to make unreacted metal salt dissolve and complete the reaction. The precipitation was then washed several times with the help of a centrifuge machine to remove the contaminants. Further, the material is collected and dried under a heating oven for 2 h under 150 °C.

4.1. Characteristics of AlO(OH) nanoparticles

Prepared material is characterized by various techniques and the product was analyzed using UV–visible optical absorption spectra recorded by a Specord-200 PLUS spectrometer from Analytic, Germany. It is a quantitative technique used to measure how much a chemical substance absorbs light. The morphology of the sample was observed by scanning electron microscopy (SEM, Zeiss Ultra-55)

Table 1
Properties of diesel, DiSOME, and blended fuel.

Property	Diesel	DSOB	DSOB + AlO(OH)20	DSOB + AlO(OH)40	DSOB + AlO(OH)60	ASTM Test Method
Calorific value, kJ/kg	43500	40165		39016		D 240
Density, kg/m^3	840	868	833.2	838.6	346.4	D287
Kinematic viscosity @ 40°C, mm^2/s	3.2	3.9	**4.2**	**4.75**	5.1	D445
Flash point, ^{0}C	56	145	**156**	**167**	175	D 92
Fire point,^{0} C	68	164	176	184	192	D 92
Cetane number	54	60	–	–	–	–
Carbon remainder, %	0.21	0.64	0.61	0.58	0.56	D 189

Table 2
Properties of biomass and composition of producer gas.

Property	Mixed biomass	Property	Composition of producer gas
Moisture content (% w/w)	11.02	CO, %	17–21
Ash content (w/w)	0.91	H_2, %	14–18
Volatile matter (%w/w)	75.8	Methane, %	2–6
Fixed carbon (%w/w)	10.99	HC, %	0.3–0.5
Sulphur (%w/w)	0.08	N_2, %	4.4–5.4
Nitrogen (% w/w)	0.17	Water vapor, %	4.9
Calorific value (cal/g)	3188	CO_2, %	9–11
Density (kg/m^3)	291	Calorific value. kJ/Nm^3	4.6

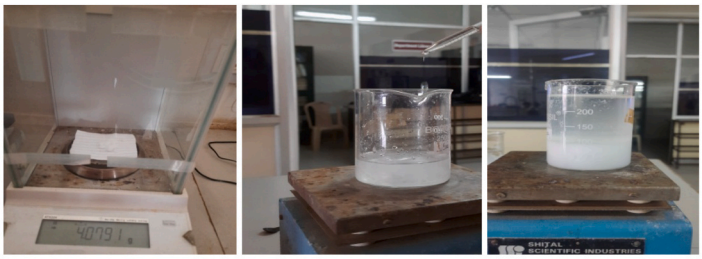

(a) Weighing of AlNO3 and NaOH (b) Titration (c) Stirring

(d) Material measurement (e) Mixing of ingredients (f) AlO(OH) nanoparticle

Fig. 2. Synthesis of AlO(OH) nanoparticles.

at an accelerating voltage of 10 kV. The crystalline structural analysis is carried out by using powder X-ray diffraction (XRD) (Rigaku smart lab RD100) and also calculating the particle size of the nanomaterial. The thermal analysis was studied by differential scanning calorimetry (DSC) (Quanta-20). Thermogravimetric analysis was carried out by TGA (SDT Q-600 TA instruments, USA). Detailed

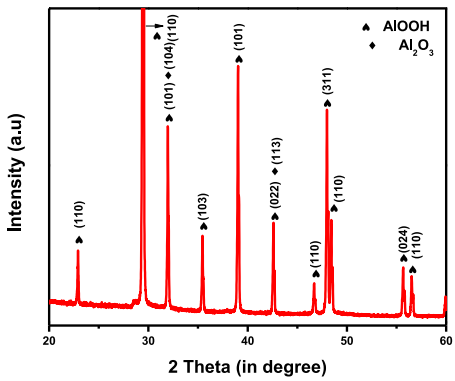

Fig. 3. XRD patterns of as-prepared AlO(OH) sample.

analysis of the characterization of nanoparticles is given in the following subsequent paragraph.

4.1.1. XRD analysis

The crystal phases of the nanoparticles were established and analyzed using X-ray diffraction (wavelength of 1.54 Å) between 20 and 60° at a scan rate of 10° min^{-1}.The peaks were very sharp, indicating good crystallinity of the compound. The XRD pattern of this material (Fig. 3) indicated the presence of mixed phases in the prepared samples. The strongest peak was at 29.5°and the second strongest peak appeared at 39.2° corresponding to the d-spacing values of 3 Å and 2.3 Å representing the planes (110) and (020) respectively of δ-AlO(OH) phase.

Further, some minor peaks appeared at different diffraction angles at 22.91°, 35.44°, 42.56°, 48.52°, and 55.68° corresponding to core planes (110), (103), (101), (311) and (024) respectively, indicates the presence of δ-AlOOH with varied composition, however two peaks at 31.99 and 42.56 are the mixed phase of Alumina (Al_2O_3) and δ-AlOOH. Two more peaks are unidentified at 46.7° and 56.7° and observed pattern well matched with the standard JCPDS number (721475). The δ-AlOOH phase is a high-pressure polymorph of the natural aluminous hydrous minerals diaspore (α-AlOOH) and boehmite (γ-AlOOH). The calculated average particle size from the graph is around 74 nm. Table 3 provides the XRD peak analysis of nanoparticles which gives information about the crystalline properties and particle size.

4.1.2. Differential scanning calorimetry (DSC)

The DSC curve of AlO (OH) scanning from 100 °C to 400 °C is shown in Fig. 4 and the heating rate was 10 °C/min. It is seen that significant two endothermic peaks appear at 276 °C and 309 °C. The first endothermic peak at 276 °C may have been due to the decomposition of aluminum hydroxide to form Al_2O_3. The second and sharp peak at 309 °C is attributed to gibbsite dihydroxylation and forms AlO (OH) as the final product. There is no endothermic peak around 110 °C for the samples to represent moisture which indicates the prepared samples are purely AlO (OH). DSC spectra confirm the presence of both Al_2O_3 and AlO (OH) in the prepared sample.

4.1.3. Thermogravimetric analysis

The thermo-gravimetric analysis is a technique used to determine the thermal stability of a substance and the number of volatile components it contains. This is achieved by observing the weight change that occurs while a sample is heated at a consistent rate. Thermo-gravimetric analysis (TGA) provides the purity and composition of materials, stability temperature of compounds, phase shift, adsorption, and desorption as well as their temperatures for drying and ignition. Authors have investigated the thermal stability of aluminum hydroxide by conducting DSC and TGA measurements. The measurements are carried out within a temperature range of 20°C–400°C, under an inert atmosphere, with a heating rate of 10 °C/min. In this instance, there is a little endothermic peak of about 100°C that is linked to the evaporation of the water content of the material. The aluminium hydroxide nanoparticles have a distinct exothermic peak at temperatures of around 276°C and 309°C (Fig. 5). During weight loss measurements using temperature (TGA), it is shown that aluminium hydroxide exhibits increased stability as the temperature rises. Up to a temperature of 368° C, there is only a minimal weight loss of 8 %, which remains rather consistent. However, beyond this point, there is a significant increase in weight loss, reaching over 63 % at around 611°C.

4.1.4. Optical studies

The absorption spectrum of the obtained AlOOH nano-particles of the as-prepared sample is given in Fig. 3. The absorption spectrum was taken from 200 to 500 nm, showing strong absorption in the UV region and a sharp peak at 235 nm (Fig. 6). This is because of the photo excitation of electrons from the valence band to the conduction band. Apart from a sharp peak, a small and broad peak centered at 296 nm was also observed. The optical band gap of the prepared AlOOH is estimated to be 5.2eV.

4.1.5. SEM image analysis

SEM image of AlO(OH) is shown in Fig. 7 provides information about the surface morphology and particle size of the prepared aluminium hydroxide NPs. The images shown at different positions and provide the formation of large granules using small NPs due to agglomeration. In Fig. 7 the particle size of the aluminium hydroxide NPs measured through the software installed in the instrument is approximately 61.1 nm which well matches with the particle size calculated from the X-ray diffraction study (74 nm). Further, Table 4 shows the amount of Aluminum, weight percent, and atomic percent in the aluminum hydroxide nanoparticles. It shows that 63.13 percent of oxygen and 36.87 percent of aluminum is present in the material weight-wise. Similarly, 74.27 and 25.73 percent of oxygen and aluminum respectively are present atomic weight-wise. Scanning electron microscope image does not show hydrogen because it does not have a K shell so SEM/EDS cannot detect very light elements like Hydrogen, Helium, etc.

Fig. 8 shows the graph of constituents of the material as per SEM testing. This graph shows electronic dispersion X-ray (EDX) results i.e., kilo electron volt (keV) vs counts per second per electron-volt (cps/eV). The percentage distribution of the elements in the composite mass, shown within the appropriate voltage range, is measured in seconds per electronvolt. X-rays are produced through the utilization of EDX in a two-step procedure. Initially, the energy imparted to the atomic electron dislodges it, resulting in the creation of a hole. Secondly, its position is filled by another electron from a higher energy shell i.e., aluminum in this case. The graph shows the presence of aluminum and oxygen but lacks hydrogen presence due to the very light weight of hydrogen and the absence of a K shell. Fig. 8 shows the percentage of the constituent in the sample as per SEM images. Table 4 generated from the EDX.

Table 3
The analysis of the XRD Peak Profile of AlOOH sample.

No.	2θ°	e.s.d.	d/Å°	e.s.d.	Height, counts	e.s.d.	FWHM°	e.s.d.	Int.I., counts°	e.s.d.	Int.W.I°	e.s.d.	Asymmetry	e.s.d.	Decay/ηLmL^{-1}	e.s.d.	Decay/ηHmH^{-1}	e.s.d.	Size/Å°
1	22.91406	0.00255	3.87799	0.00043	715.4	19	0.1033	0.0028	90.7	1.51	0.1268	0.0055	2.779	0.371	0.345	0.065	0.583	0.141	819.6982
2	29.45087	0.00162	3.03043	0.00016	23569.1	153.1	0.068	0.0025	2474.31	41.61	0.105	0.0024	0.781	0.053	1.4	0.13	0.426	0.067	1261.34
3	31.97082	0.00196	2.79709	0.00017	2856.6	45.3	0.0972	0.0021	378.39	3.54	0.1325	0.0033	2.622	0.304	0.547	0.038	0.965	0.106	887.6773
4	35.45883	0.00205	2.52953	0.00014	1118.6	27.9	0.1093	0.002	150.24	1.67	0.1343	0.0048	3.043	0.335	0.261	0.042	0.799	0.112	797.2483
5	39.04055	0.00152	2.30531	0.00009	3812.9	52.2	0.1083	0.0015	521.26	3.59	0.1367	0.0028	3.549	0.327	0.298	0.021	0.988	0.091	812.7879
6	42.60653	0.00191	2.12025	0.00009	1443.7	33.3	0.1079	0.0018	189.62	1.98	0.1313	0.0044	3.721	0.439	0.241	0.035	0.828	0.122	825.2975
7	46.70018	0.00312	1.94348	0.00012	507.5	18.8	0.1106	0.0028	70.61	2.13	0.1391	0.0093	2.147	0.3	0.551	0.074	0.308	0.277	817.4045
8	46.92299	0.0162	1.93477	0.00063	28.1	1.9	0.1111	0.0435	3.93	1.62	0.1399	0.0671	2.147	0.3	0.551	0.074	0.308	0.277	813.8149
9	47.99991	0.00137	1.89385	0.00005	3480.3	54.9	0.1091	0.0012	475.85	3.22	0.1367	0.0031	2.979	0.217	0.359	0.022	0.748	0.074	832.8386
10	48.43168	0.00232	1.87797	0.00008	1597.8	35.3	0.0944	0.0024	225.48	2.48	0.1411	0.0047	1.81	0.233	0.945	0.066	0.789	0.1	963.3837
11	55.67344	0.00211	1.64962	0.00006	870.3	26.9	0.1115	0.002	129.18	1.29	0.1484	0.0061	2.511	0.271	0.513	0.042	0.859	0.102	841.6038
12	56.5396	0.0025	1.62639	0.00007	682.3	23.6	0.1161	0.0023	103.24	1.23	0.1513	0.007	2.404	0.287	0.434	0.05	0.844	0.116	811.7061
13	59.94288	0.00334	1.54192	0.00008	330.9	14.4	0.1195	0.0033	44.96	1.03	0.1359	0.009	3.596	0.662	0.003	0.089	0.733	0.213	801.4568
14	61.00108	0.00206	1.51769	0.00005	178.9	10.9	0.0804	0.0054	21.03	0.9	0.1176	0.0122	0.526	0.151	1.55	0.116	0.132	0.245	1197.399
15	61.65819	0.00358	1.50308	0.00008	402.2	17.4	0.1199	0.0033	60.71	1.14	0.151	0.0094	2.416	0.401	0.311	0.081	0.811	0.167	805.6835
16	62.39527	0.00267	1.48708	0.00006	472.3	18.7	0.1275	0.0022	69.23	1.09	0.1466	0.0081	1.989	0.201	0.126	0.067	0.419	0.116	761.0653
17	63.57949	0.00258	1.46221	0.00005	588.4	21.6	0.1128	0.0025	84.26	1.17	0.1432	0.0072	2.696	0.361	0.32	0.055	0.888	0.132	865.242
18	66.72433	0.00167	1.40072	0.00003	523.3	20.4	0.1155	0.0026	78.81	1.1	0.1506	0.008	4.428	0.571	0.255	0.051	1.399	0.117	859.7542
19	68.72579	0.00382	1.36473	0.00007	260.6	13.4	0.1218	0.0031	36.59	0.88	0.1404	0.0106	1.639	0.232	0.179	0.108	0.33	0.163	825.423
20	70.50341	0.00756	1.33461	0.00012	108.2	7.6	0.1338	0.0068	17.17	0.8	0.1587	0.0185	1.855	0.504	0.371	0.208	0.218	0.348	759.5556
21	72.5558	0.00467	1.30183	0.00007	194.8	11.8	0.1214	0.006	33.27	0.87	0.1708	0.0148	2.478	0.595	0.456	0.121	1.268	0.203	847.8597
22	74.89124	0.00944	1.26692	0.00014	90.5	6.9	0.1236	0.0087	13.97	0.76	0.1544	0.0202	1.303	0.438	0.447	0.278	0.476	0.348	845.6024
23	77.83922	0.00359	1.22614	0.00005	174.1	11	0.1029	0.0054	27.82	0.75	0.1598	0.0144	2.928	0.689	0.691	0.126	1.523	0.171	1036.429
24	81.42087	0.00634	1.18101	0.00008	139.4	10.2	0.1291	0.0067	24.76	0.72	0.1775	0.0182	1.491	0.343	0.654	0.152	0.769	0.209	848.0235
25	82.41959	0.00332	1.16921	0.00004	367.4	17.3	0.1266	0.0035	63.88	0.89	0.1739	0.0106	1.719	0.222	0.507	0.068	0.969	0.111	871.3436
26	83.70138	0.00685	1.15454	0.00008	72	5.9	0.1294	0.0104	13.56	0.71	0.1883	0.0253	1.98	0.479	0.555	0.257	1.237	0.373	861.1378
27	86.4929	0.01021	1.12429	0.00011	81.5	5.9	0.1365	0.0116	15	0.76	0.1842	0.0226	1.899	0.727	0.668	0.244	0.63	0.387	834.5198

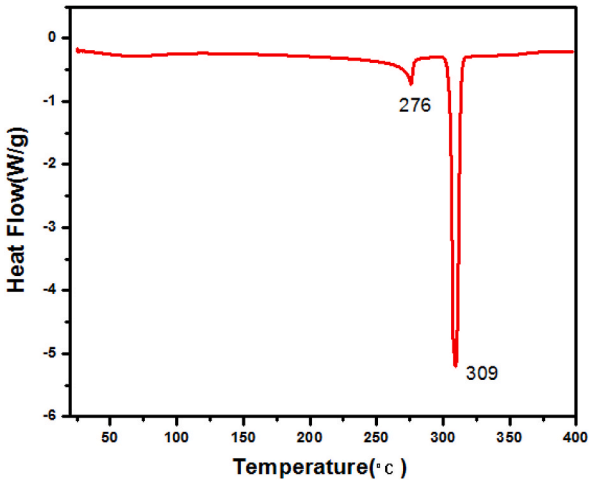

Fig. 4. DSC curve of (AlOOH) powder.

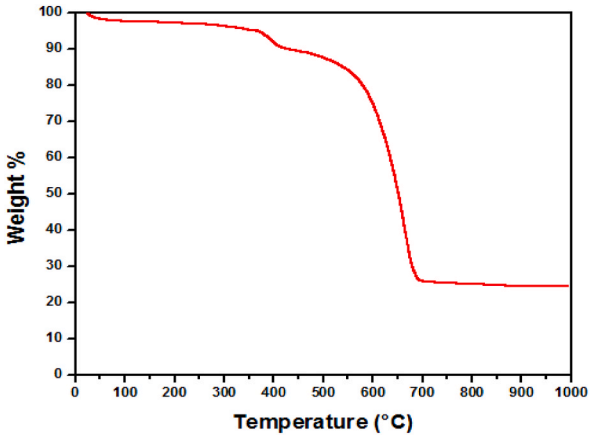

Fig. 5. Thermo-gravimetric graph.

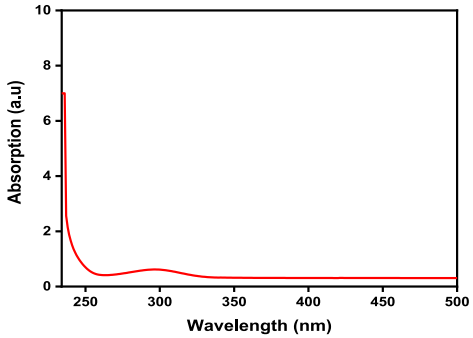

Fig. 6. Optical absorption study of AlOOH nanoparticles.

5. DSOB and AlO(OH) nanoparticles blend preparation and stability study

In the first step, the AlO(OH) nano-particles are weighed to a predetermined mass fraction and were added to DiSOME.Nano-particles are dispersed in a DiSOME using an ultrasonicator set at 40 kHz, 120W for 1min. The use of an ultrasonicator is good for

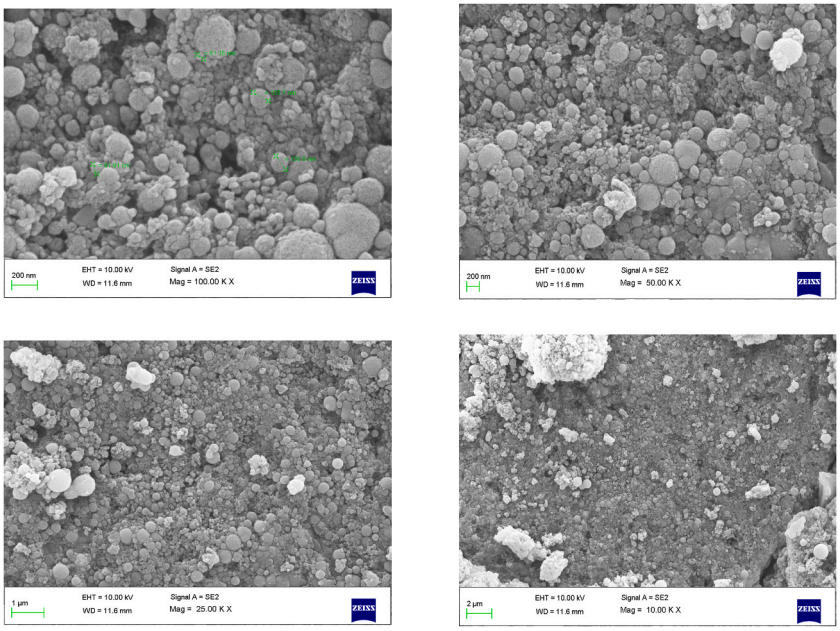

Fig. 7. SEM images of the AlO(OH).

Table 4
Constituents of Material synthesized as per SEM results.

Elements	Line type	Weight %	Atomic %
O	K series	63.13	74.27
Al	K series	36.87	25.73
Total		100	100

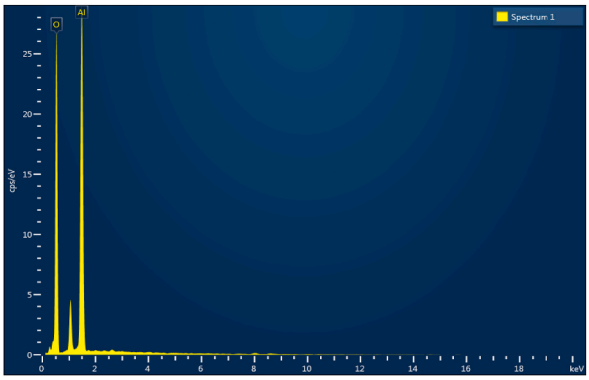

Fig. 8. SEM results.

dispersing the AlO(OH) nano-particles in biodiesel, as it helps in agglomerated nano-particles back to nano-meter size. AlO(OH) nano-particles – DiSOMEfuel is prepared, and this mixture is denoted as DiSOME + AlO(OH)20. Similarly, other blends DiSOME + AlO(OH) 40 and DiSOME + AlO(OH)60 were prepared. However, the present study was limited to 60 ppm, because more concentration of metal nanoparticles in the biodiesel may lead to unsafe occurrences on the engine cylinder liners and piston surface [24]. This is essential to inspect whether AlO(OH) nanoparticles dispersed or not in the biodiesel due to agglomeration. Nanofluids stability can be achieved by the addition of surfactant. The literature suggested that metal-based nanoparticles and non-metals can be dispersed in the fluids with/without surfactant. In addition, thermodynamically, it is observed that only emulsion fuels are in unbalanced and unstable conditions, and hence in such a blending two immiscible phases may be bound to take place [24].

In this present study, the stability test was checked, using known quantity of AlO(OH) nano-particles blended with known quantity of biodiesel in a transparent beaker at steady conditions and stirred mechanically using sonicator. After sonication the nanoblended

fuel was kept for 48 h and observed no settling. This may because, dairy scum oil is consisting of 32–35 % oleic acid and is an integral part of biodiesel fuel. This oleic acid enhances the nanofluids stability [64].

6. Experimental setup

The experimental setup comprises a 1-cylinder, 4-stroke compression ignition (CI) engine coupled with an eddy current-type dynamometer for loading. The engine was coupled with a downdraft gasifier with a cooling and cleaning system. Fig. 9 show the photographic view of the engine-gasifier system. The engine was operated at a steady speed of 1500 revolutions per minute. The specification of the CI engine and down draft gasifier is given in Tables 5 and 6. The engine had a hemispherical combustion chamber and matched with a 3-hole, 0.25 mm hole size nozzle. The signals from different sensors are connected to a computer through an engine indicator to monitor performance and combustion parameters. Sensors are used for interfacing airflow, fuel flow, temperatures, and load measurement. CI engine is also made up of facilities to measure airflow, fuel flow, temperatures, and loads. Rotameters are used for cooling water and water flow measurement of calorimeter. The air and fuel flow rates were recorded on a volumetric basis. Engine cooling was achieved by water circulation through the jackets of the engine block and cylinder head. Engine performance analysis software-based Labview package, Engine soft is provided to evaluate the engine performance.

Dual fuel engine performance with biodiesel and producer gas combination was improved by the addition of nanoparticles. In the first step, required AlO(OH) nano-particles are weighed to a predetermined mass fraction and mixed in a known quantity of DiSOME. The nano-particles dispersed in a DiSOME using an ultrasonicator set at a frequency of 40 kHz, 120W for 1min, thereby uniform mixture is achieved. DiSOME with nanoparticles blended fuel is prepared and this mixture is denoted as DiSOME + AlO(OH)20. Similarly, other blends DiSOME + AlO(OH)40 and DiSOME + AlO(OH)60 were prepared. However, the present study was limited to 60 ppm, because more concentration of metal-based nanoparticles in the biodiesel may lead to unsafe occurrences on the engine cylinder liners and piston surface [24].

Producer gas is generated by a downdraft gasifier and the gas flow rate was measured using a calibrated venturimeter equipped with a digital gas flow meter. The engine operating parameters for various modes of engine operation are displayed in Table 7. For a fixed brake power an additional quantity of biodiesel is consumed as its energy content is noticeably lower and its kinematic viscosity is larger. Biodiesel quantity was increased by adjusting the speed of the governor so that a stable speed was maintained. It is noticed that specific fuel consumption (SFC) for diesel operation is 260 g/kWh while for DiSOME it is 325 g/kWh at 80 % load. During the experimentation, regulated emission characteristics were measured using a HARTRIDGE smoke meter and five gas analyzers (Model Gasboard-5020, A DELTA 1600 S). The producer gas flow rate was not controlled, and the airflow rate was controlled to attain smooth engine operation. Fig. 10 illustrates the methodology adopted during the experimentation.

7. Results and discussions

In this part impact of various nano-particles viz., Al_2O_3, MWCNT, and AlO(OH) blended fuel on the combustion behavior and emissions of a dual-fuel CI engine has been investigated in three phases. In the first phase, AlO(OH) NP was synthesized, characterized and analyzed in the previous section. However, in this section, i.e., second stage of the work, the effect of AlO(OH) NP dosage on the overall performance of a producer gas-powered diesel engine was examined and a better proportion of NP was selected. In the subsequent third phase, the effects of 60 ppm concentrations of different nanoparticles, such as multi-walled carbon nanotubes (MWCNT), Aluminum oxide (Al2O3), and Aluminium oxyhydroxide (AlO(OH)), on the combustion and emission characteristics of a single cylinder four-stroke direct injection diesel engine operating in dual fuel mode with dairy scum oil methyl ester (DiSOME) - producer gas were investigated. A comprehensive examination of trial testing is presented in the next section.

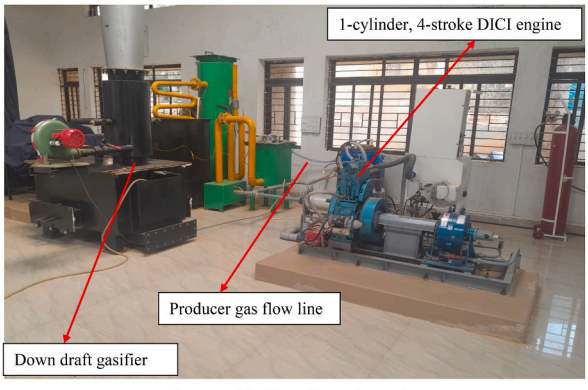

Fig. 9. Experimental setup.

Table 5
Shows the specifications of the experimental test rig.

Sl. No.	Parameters	Specification
1	Machine Supplier	Apex Innovations Pvt Ltd, Sangli. Maharastra State.
2	Engine Type	Single cylinder four stroke water cooled direct injection TV1 CI engine with a displacement volume of 662 cc, compression ratio of 17:1, developing 3.7 kW at 1500 rev/min TV1 (Kirolsker make)
3	Software used	Engine Soft
4	Nozzle opening pressure	200–225 bar
5	Governor type	Mechanical centrifugal type
6	Cylinder diameter (Bore)	0.0875 mtr
7	Stroke length	0.11 mtr
8	Combustion camber	Open Chamber (Direct Injection) with hemispherical cavity
9	Eddy current dynamometer	Model:AG – 10, 7.5 KW at 1500 to 3000 RPM, and Water flows through the dynamometer during the use

Table 6
Specification of the downdraft gasifier.

Type	Downdraft gasifier
Rated capacity	15000 kcal/h
Rated gas flow	15Nm^3/hr
Average gas calorific value	1000 kcal/m^3
Rated woody biomass consumption	5–6 kg/h
Hopper storage capacity	40 kg
Biomass size	10 mm (Minimum) 50 mm (Maximum)
Moisture content (DB)	5–20 %
Typical conversion efficiency	70–75 %

Table 7
Engine operating parameters.

Mode of engine operation	Fuels used with and without nanoparticles	IT (deg. bTDC)	IP (Bar)	CR	Nozzle used
Dual fuel (DF) operation	Diesel-PG combination DiSOME - PG combination	27 27	205 230	17.5	3 holes, 0.25 mm dia.

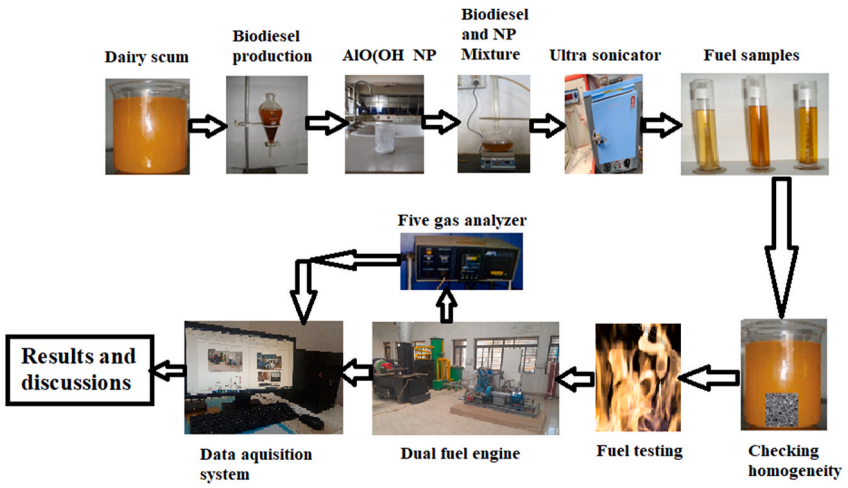

Fig. 10. Test flow diagram.

7.1. Optimization AlO(OH) nano-particle proportion in a biodiesel-producer gas combination

7.1.1. Performance characteristics

The disparity of brake thermal efficiency (BTE) relating to maximum load is presented in Fig. 11. It is examined that the DiSOME-PG process presented lowered BTE by 14.2 % than tothe diesel-PG process. This might be because ofthe combined influence of biodiesel and producer gas, both pilot fuel and inducted producer gas have lower energy content, and biodiesels higher viscosity and density lowers the performance. However, the inclusion of AlO(OH) NPs in a DiSOME biodiesel boosts the dual fuel operation's heat release rate because of the nanoparticles' higher surface-volume ratio and catalytic activity, which intensifies the kinetics of the chemical reaction. AlO(OH) nano-additives may respond to biodiesel combustion at higher loading conditions, which in turn encourages combustion [24,65]. AlO(OH) nano-additive contains inbuilt oxygen and hydrogen which provide oxygen and hydrogen during combustion. The inbuilt hydrogen of a nanoparticle increases leanness which has a greater influence on performance.

Further, a small hydrogen quantity enhances the oxygen-reaching ability and homogeneity, because hydrogen has a greater diffusion co-efficient [66]. This could also amplify the oxidation process and flame speed leading to an increased combustion rate. In addition, AlO(OH) nano-additive has a crystalline structure and acceptable burning temperature, this in turn helps in speedy oxidation, and improved fuel burning rate. Hence, it is revealed that there is a relationship between the proportion of nano-particle addition in biodiesel and the power output. Results showed that DiSOME-PG operation with 20 ppm,40 ppm, and 60 ppm AlO(OH) and without nano-addition resulted in decreased BTE by 13.6 %, 9.4 %, 2.9 %, and 14.6 % respectively than diesel-based dual fuel operation.

Fig. 12 displays the fuel replacement for several fuel combinations when operating at maximum power output. The engine study focuses on fuel combinations, which are both sustainable fuels, allowing for flexibility in altering the fuel replacement ratio. Under the same operating conditions, the diesel-producer gas operation exhibited higher fuel substitution values than the DiSOME-producer gas combination. The observed trend may be caused by fuel factors such as composition, type, cetane number, viscosity, and calorific value. When AlO(OH) nanoparticles were introduced to biodiesel-PG, there was a little increase in fuel substitution compared to neat DiSOME-PG operation. Enhanced oxygen and hydrogen supply with the addition of nanoparticles to biodiesel improves the combustion of highly volatile fuel with producer gas [3]. Lessening the fuel combination's leanness is one potential way to enhance combustion. Therefore, the pilot fuel supply was slightly raised to enhance the mixture's quality. Results showed that increased nano-particle dosage increases the fuel substitution rate due to adequate utilization of nano-particle inbuilt oxygen and hydrogen. Both adding nanoparticles and increasing pilot fuel can improve the combustion of producer gas. Results showed that DiSOME-PG operation with 20 ppm, 40 ppm, and 60 ppm AlO(OH) and without nano-addition resulted in decreased fuel substitution by 3.4 %, 2.5 %, 1.8 %, and 5.9 % respectively than diesel-based dual fuel operation.

7.1.2. Emissions characteristics

The results of the emission characteristics of the AlO(OH) NP additives in the biodiesel-PG combination are examined in the section follows.

Smoke emissions were produced because of the inferior properties of the fuel. Smoke opacity variation concerning maximum load is shown in Fig. 13. Observations indicated that the diesel-PG combination reduced the amount of smoke levels in the exhaust by 26.6 % compared to the DiSOME-PG operation. This can be attributed to inadequate combustion resulting from the inferior properties of both DiSOME and PG. Lowered combustion temperature and inadequate air-fuel mixture formation may also be the reason. However, the use of AlO(OH) NP blended DiSOME during dual fuel operation has the potential to reduce the amount of smoke emitted i.e., The use of AlO(OH) nanoparticles in biodiesel-PG operation resulted in lower smoke emissions than that of neat biodiesel-PG operation.

This is due to the higher surface area-volume ratio and the catalytic activity of the AlO(OH) NPs. In addition, AlO(OH) nanoparticles have a relatively greater surface-area-to-volume ratio, making them ideal catalysts and the presence of oxygen and hydrogen content in blended fuel positively influences the combustion rate due to improved air-fuel mixture quality and enhanced hydrogen flame speed. In several studies, the additional hydrogen and oxygen provided by the inbuilt nanoparticles have been accentuated as the cause behind the considerable reductions in smoke emissions [24,66]. Results showed that, at DiSOME-PG operation with 20 ppm, 40

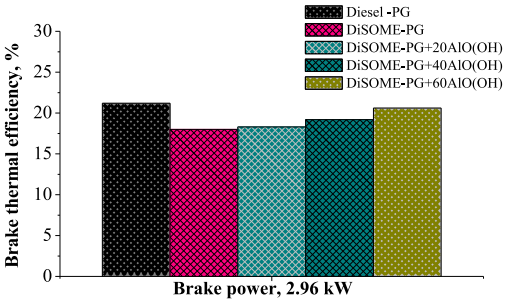

Fig. 11. Influence AlO(OH) nanoparticles on the BTE.

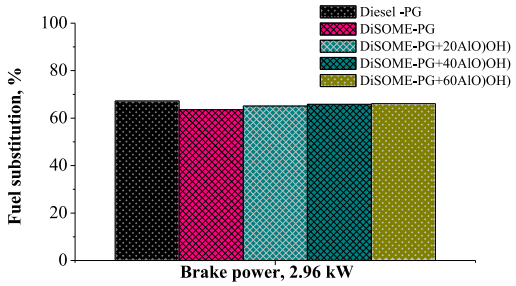

Fig. 12. Influence AlO(OH) nanoparticles on the fuel substitution.

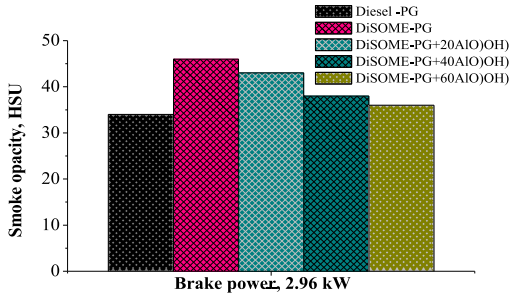

Fig. 13. Influence AlO(OH) nanoparticles on the smoke opacity.

ppm, and 60 ppm AlO(OH) and without nano-addition resulted in increased smoke levels by 20.9 %, 11.8 %, 5.8 %, and 35.8 % respectively compared to the operation diesel based dual fuel operation.

Carbon-based emission level variations with different fuel combinations are demonstrated in Figs. 14 and 15.The HC and CO levels are elevated in the biodiesel-PG combination compared toin diesel-PG operation because of the efficient production of the air-fuel mixture with diesel. Improved blending of diesel with an air-producer gas mixture is the reason for the pattern of the observed result, leading to enhanced combustion. Reduced HC and CO emissions were noticed with AlO(OH) NP blended biodiesel-based dual fuel operation and the desirable effect of AlO(OH) NP addition to fuel leads to superior combustion due to inbuilt oxygen and hydrogen of nanoparticle. Nano-particle studies on EDX showed the presence of 74.27 % oxygen, in turn, improves the oxidation rate and the hydrogen content of nanoparticles helps to enhance the combustion rate due to the increased flame speed of hydrogen.

Results showed that DiSOME-PG operation with 20 ppm, 40 ppm, and 60 ppm AlO(OH) and without nano-addition resulted in increased HC levels by 34.2 %, 23.6 %, 12.5 %, and 42.8 % respectively than diesel-based dual fuel operation. CO levels increased by 23.4 %, 16.5 %, 10.6 %, and 31.5 % compared to the diesel-based dual fuel operating at 80 % load. Moreover, it has been noted that the

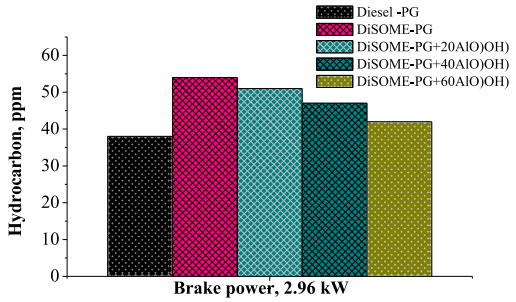

Fig. 14. Influence AlO(OH) nanoparticles on the HC emission.

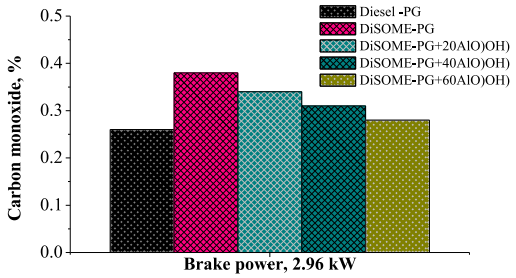

Fig. 15. Influence AlO(OH) nanoparticles on the CO emission.

presence of 60 ppm nanoparticles in biodiesel, when dispersed well, leads to improved catalytic activity and air-fuel mixture formation due to the appropriate viscosity of biodiesel at this concentration. This, in turn, aids in reducing HC and CO emissions. The observed trend can be attributed to the greater surface area-volume ratio and superior catalytic activity of AlO(OH) NPS. Similar observations were made by Srinivasa Rao and Anand [2]. However, the additional nanoparticle is limited to 60 ppm because of engine safety. Results showed that DiSOME-PG operation with 20 ppm, 40 ppm, and 60 ppm AlO(OH) and without nano-addition resulted in increased NOx levels by 34.2 %, 23.6 %, 12.5 %, and 42.8 % respectively than diesel-based dual fuel operation.

Nitric oxide (NOx) emissions at peak load are illustrated in Fig. 16 for different fuel combinations. For identical conditions, the diesel-PG combination provided greater NOx emissions by 41.2 % than the DiSOME-PG operation. It can be because diesel has better qualities and therefore promotes better mixture formation and higher combustion temperatures.Furthermore, the increased NOx emissions in diesel-PG operation can be attributed to enhanced premixed combustion rather than the diffusion combustion phase, as stated by Banapurmath et al. [11]. The demonstrated results with the addition of nanoparticles to the biodiesel fuel improve properties like viscosity, density, and calorific value [67,68]. Also, the addition of AlO(OH) nanoparticles to biodiesel enhances the mixture quality and increases the flame speed due to the presence of inbuilt oxygen and hydrogen which in turn enhances the premixed combustion phase. Normally, the catalytic activity and larger surface-volume ratio of NP accelerate the rate of combustion, resulting in greater amounts of NOx emissions than pure biodiesel-PG. NOx emissions for 20 ppm, 40 ppm, and 60 ppm AlO(OH) addition to the DISOME-PG combination were found to be reduced by 36.5 %, 28.6 %, 15.8 %, and 42. 2 % respectively, than diesel-based dual fuel operation. This could be attributed to the improved oxidation rate, mixture quality, flame speed, and enhanced catalytic action achieved with dual fuel operation using 60 ppm AlO(OH) in biodiesel, as compared to other fuel combinations.

7.2. Influence of type of nanoparticle on the performance of biodiesel-producer gas-powered diesel engine

7.2.1. Performance characteristics

Fig. 17 illustrates the fluctuation of BTE for various fuel combinations, both with and without NPs of diverse origins. Owing to higher viscosity lower volatility, and other inferior properties of both biodiesel and PG, the dual fuel engine operated on DiSOME-PG operation provided deprived BTE by 13.6 % compared to diesel-PG combination. For the same fuel combination with a 60 ppm dosage of nanoparticles, MWCNT and Al2O3 NP-based dual fuel process resulted in reduced BTE by 5.45 % and 2.01 % respectively than the operation with AlO(OH) NPs at 80 % load. However, DiSOME-PG operation with 60 ppm AlO(OH) nanoparticles resulted in a 5.8 % lower BTE than diesel-PG operation. This may be attributed to the fact that AlO(OH) nanoparticles provide both hydrogen and oxygen during combustion. This in turn increases oxidation rate and flame prorogation. Common properties of nanoparticles are marginally

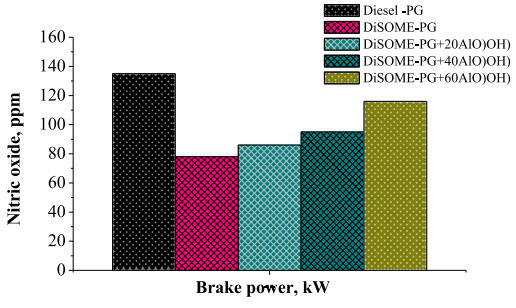

Fig. 16. Influence AlO(OH) nanoparticles on the NOx emission.

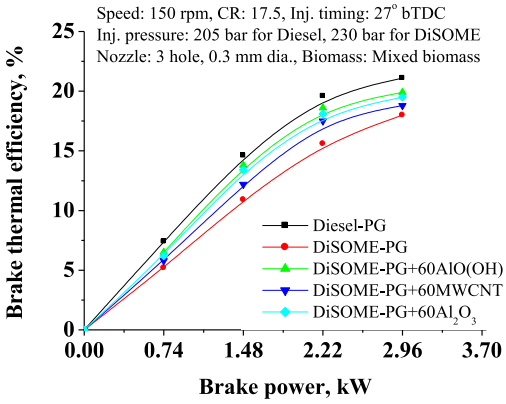

Fig. 17. Effect of different nanoparticles on the variation of BTE.

the same, but the influence of inbuilt hydrogen and oxygen of AlO(OH) nanoparticles makes differences in thermal efficiency compared to Al_2O_3 and MWCNT. Further, it could be because greater catalytic action of AlO(OH) NPs may lead to better combustion of liquid fuel along with gaseous fuel. It is observed from.

Fig. 18 that the fuel consumption of nanoparticles blended biodiesel powered dual fuel operation decreases with the addition of nanoparticles in biodiesel against the neat biodiesel-PG operation due to the existence of hydrogen and/or oxygen in nano-particles. The utilization of NP-dispersed biodiesels in dual fuel operation resulted in greater BTE than neat biodiesel-PG operation. This improvement can be attributed to the combined impact of micro-explosion and secondary atomization [2,69]. AlO(OH) NPs have enhanced combustion characteristics and can be utilized as catalysts in the combustion of DiSOME-PG mixtures. This leads to an increased oxidation rate and improved volumetric efficiency, exceeding the performance of Al2O3 and MWCNT NPs in dual fuel operations. Generally, AlO(OH) nano-size is marginally the same as that of Al_2O_3 and MWCNT particles, as a result, they possess a larger surface area and reactive surfaces, which enhance their chemical reactivity and make them effective catalysts [2,70]. Dual fuel operation with MWCNT and Al2O3 provided lower BTE than the operation with AlO(OH). This may be due to the absence of oxygen in MWCNT and hydrogen in Al2O3 nano-articles.

Fig. 18 illustrates the changes in EGT for several fuel combinations, both with and without nanoparticles from diverse sources.EGT is augmented with an increase in load caused by more fuel accumulation within the engine cylinder and incomplete combustion. Foridentical operating conditions, the biodiesel-PG combination provided increased EGT by 21.82%thanthe diesel-PG combination. The potential cause may be attributed to inadequate combustion of biodiesel in conjunction with PG. Also, inadequate mixture formation attributable to the inferior properties of DiSOME and PG combination is responsible. During biodiesel-based operation, the combustion temperature is lower, and it results in unburnt HC, this subsequently undergoes burning through the diffusion combustion phase. The characteristic of premixed combustion during biodiesel-PG-based operation is lower than in diesel-based dual fuel process [11]. However, this premixed combustion can be improved by the addition of nanoparticles having catalytic action in a pilot fuel. The addition of nanoparticles provides catalytic action during combustion and hence results showed improved pre-mixed combustion of fuel combination and observed increased combustion rate. Therefore, for the same 60 ppm of nano-particle addition,Al2O3 and MWCNT nanoparticles in a DiSOME biodiesel provided increased EGT by 9.64 % and 5.86 % respectively than the same fuel operation with AlO(OH) nanoparticles. The properties of nanoparticles and composition also affect the performance of the biodiesel-PG operation. Hence 60 ppm of AlO(OH) provided reduced EGT due to the presence of oxygen and hydrogen in the AlO(OH) nanoparticles. It could be owing to increased flame speed and improved oxidation of fuel amalgamation attributed to oxygen existence in a nanoparticle.

7.2.2. Emission characteristics

Fig. 19 illustrates the changes in smoke opacity levels in the tailpipe concerning brake power for different fuel mixtures with and without nanoparticles. The smoke opacity decreased by 34.8 % in diesel-PG operation than DiSOME-based dual fuel operation under identical conditions. This was owing to the poor combustion caused by the larger molecular structure, higher viscosity, and density of biodiesel. Furthermore, the decreased combustion temperature is a result of the interaction between biodiesel and producer gas. The decrease in oxygen levels during combustion due to the substitution of air with producer gas may potentially be a contributing factor. However, the addition of 60 ppm Al2O3 and MWCNT nanoparticles ina DiSOME, a producer gas combination, provides 10.8 % and 18.5 % enhanced smoke opacity compared to the same fuel combination with60 ppm AlO(OH) nanoparticles. It could be due to the better burning quality of AlO(OH) nanoparticles compared to other nanoparticles, which assists in rapid oxidation, improved flame propagation, and combustion rate caused by the greater catalytic action. The presence of inbuilt oxygen and hydrogen in AlO(OH) nanoparticles catalyzes oxidation and enhances the combustion rate [2]. In addition, a small quantity of hydrogen presence in AlO (OH) nanoparticles enhances the oxygen-reaching ability. This is enhanced by the higher diffusion coefficient of hydrogen, resulting in

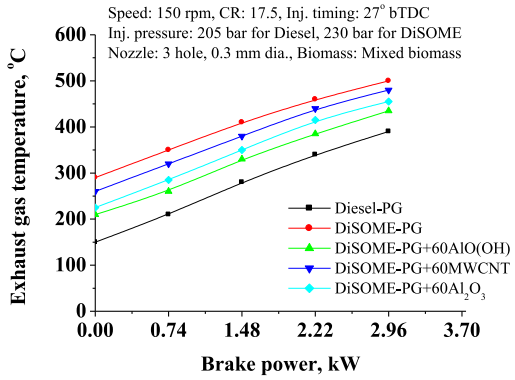

Fig. 18. Effect of different nanoparticles on the variation of EGT.

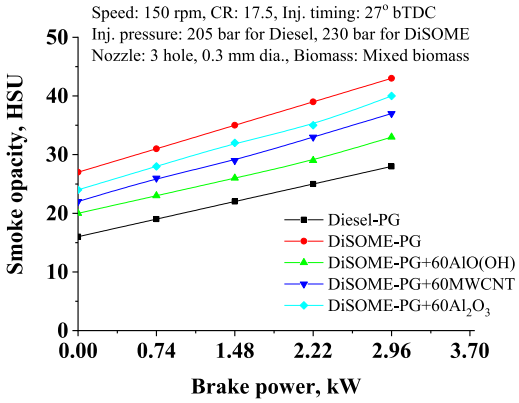

Fig. 19. Effect of different nanoparticles on the variation of smoke opacity.

improved combustion as stated by Ref. [66].Yet, utilizing Al2O3 for dual fuel operation provided slightly reduced smoke levels than MWCNT, attributed to the enhanced oxidation rate.

Figs. 20 and 21 displays carbon-based emission levels at different engine loads for DiSOME and producer gas combinations with and without various nanoparticles. The incomplete combustion of the fuel combination used is responsible for the emissions of HC and

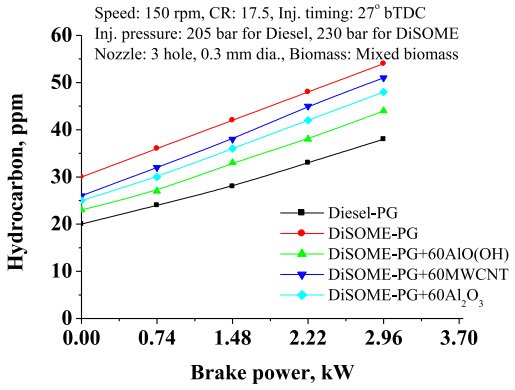

Fig. 20. Effect of different nanoparticles on the variation of HC emission.

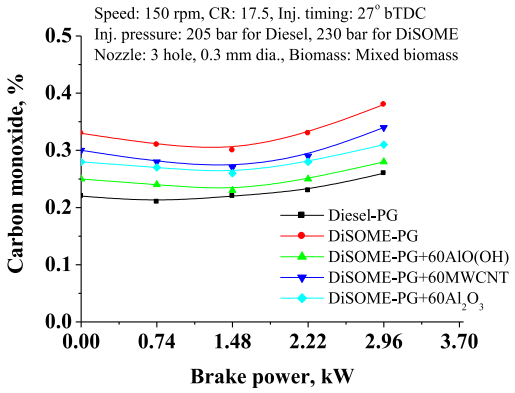

Fig. 21. Effect of different nanoparticles on the variation of CO emission.

CO. These emissions tend to rise with higher loads. It could be owing to less availability of oxygen and greater fuel consumption at higher loads. However, in a dual fuel operation, engine operation suffers from oxygen deficiency resulting from the substitution of air with producing gas. Hence it is noticed that increased HC and CO emissions by 29.6 % and 31.5 % respectively to diesel-PG operation and this may be caused by poor PG and biodiesel characteristics, as well as an inappropriate spray pattern because of the biodiesel's higher viscosity and density, lower oxygen concentration, and lower burning temperature by. However, the nano particle's introduction to the DiSOME-PG mixture results in increased homogeneity and vaporization enhancement caused by the better-burning properties of the nano-particles. It is evident that XRD of AlO(OH) nanoparticle, reveals that, the AlO(OH) nano-particle is crystalline and this in turn assists in the fast burning of fuel combination. Further, the acceptable size of nanoparticles encourages secondary fuel atomization [30]. This amplifies the reactants mixing rate and assures better combustion completeness. Oxygen and hydrogen existence and greater catalytic activity enhance the combustion and lower the formation of HC and CO emissions [67].

Further, for same the fuel combination and the same proportion of nanoparticles (60 ppm), dual fuel operation with DiSOME-PG with Al2O3 and MWCNT nanoparticles resulted in increased HC emissions by 13.82 % and 5.8 % respectively than the same fuel operation with AlO(OH) nanoparticles. Similarly, the same fuel combination with Al2O3 and MWCNT nanoparticles, provided increased CO emissions by 18.4 % and 8.5 % respectively compared to the same fuel operation with AlO(OH) nanoparticles has been observed. But AlO(OH) nanoparticles blended DiSOME-PG operation lowered HC and CO emissions by 18.4 % and 8.2 % compared to neat DiSOME-PG operation. However, MWCNT has no oxygen and Al2O3 has no hydrogen group in their structure, therefore, AlO(OH) nanoparticles are more effective than the other two nano-particles.

Nitric oxide (NOx) emissions concerning brake power for different fuel mixtures, both with and without the use of nanoparticles are shown in Fig. 22.When using the identicalPG induction, dual fuel operation with diesel-PG produced 38.46 % more NOx emissions than the DiSOME-PG combination. This may be attributed to the enhanced pre-mixed combustion phase resulting from variations in the chemical energy provided to the engine. However, for the same proportion of nanoparticles (60 ppm),in addition to the DiSOME-PG combination, Al2O3, and MWCNT-based dual fuel operation resulted in decreased NOx levels by 21.8 % and 12.6 % respectively than same biodiesel-based dual fuel mixtures with AlO(OH) addition. It might be because adding AlO(OH) NPs improves the mixture's

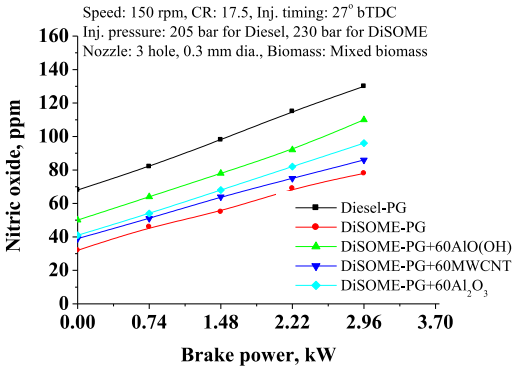

Fig. 22. Effect of different nanoparticles on the variation of nitric oxide.

quality, homogeneity, and flame speed as well as hydrogen's wider flammability limit, which raises the temperature of combustion. However, AlO(OH) nanoparticles enhance the oxygen availability, and properties of nano-particles like catalytic action enhance the combustion temperature leading to increase cylinder pressure. Additionally, by adding NPs to DiSOME, the fuel mixture becomes leaner with gaseous fuel, resulting in a sufficient ignition delay, which raises the pressure inside the cylinder. The presence of oxygen and hydrogen in AlO(OH) nanoparticles advances fuel combination burning rate leading to lower combustion duration. As far as AlO (OH) addition to DiSOME is concerned, it resulted in lowered NOx by 15.3 % than diesel-PG operation and amplified by 28.2 % to neat DiSOME-PG operation. When using dual fuel with a DiSOME-PG combination without adding NPs, the fuel combination might not burn through entirely during the pre-mixed combustion phase, which would lower the amount of NOx in the exhaust.

7.2.3. Combustion characteristics

Fig. 23 illustrates the change in ignition delay (ID) as a function of brake power for various fuel mixtures, both with and without the presence of nanoparticles. The ID was determined by measuring the time (in milliseconds) between the start of injection and the change in pressure rise on the pressure versus crank angle diagram. It is assumed that the ID decreases as brake power increases for all investigated fuel mixtures. This is due to increased gas temperature within the engine cylinder resulting from the intensified amount of fuel burning inside the cylinder. Under identical operational circumstances, dual-fuel operation with DiSOME-PG combination provided amplified ID by 10.8 % to diesel-PG combination. The reason for this could be attributed to the increased amount of highly viscous biodiesel and PG involved in the combustion process. This development can be attributed to alterations in the quality of the air-PG combination and reduced mixing rates caused by using biodiesel. Therefore, poor air-fuel mixing may tend to enhance the delay period. It is observed that, during dual fuel operation, the addition of nanoparticles in a biodiesel improves atomization and oxidation rate leading to a lowered delay period. This phenomenon may be attributed to the increased combustion resulting from the higher oxidation and catalytic activity induced by the nano-particle. Results showed that ID for the same dosage of nanoparticles (60 ppm), DiSOME-PG operation with Al2O3 and MWCNT nanoparticles was found to be increased by 1.6 % and 4.5 % respectively compared to the operation with AlO(OH) nano-particles. However, with addition of AlO(OH) in the DiSOME-PG combination resulted in an amplified ID of 3.8 % than diesel-PG operation and lowered by 7.4 % to DiSOME-PG operation. This may be due to the occurrence of both oxygen and hydrogen in the AlO(OH) nanoparticle, this in turn provides better oxidation and increased flame speed. Hydrogen can boost the pace of air-fuel mixing due to its stronger oxygen-reaching capacity resulting from its greater diffusion coefficient, leading to enhanced combustion [66].

Fig. 24 depicts the correlation between brake power and combustion duration (CD) for various fuel combinations, both with and without nanoparticles, at 80 % load. CD is defined as the duration from the ignition of combustion (SOC) until when 90 % of the total heat is released. The amplified CD has been observed with increased power output. It is due to enhanced fuel quantity injected. For similar operating circumstances, the diesel-PG operation resulted in lower CD by16.2 % compared to the operation with DiSOME-PG combinations. The reason for this is the substandard characteristics of the DiSOME and PG mixture, as well as inadequate combustion. However, nano-particle addition to DiSOME lowers the combustion duration due to reduced ID and enhanced cetane number [67].As a result, the burning rate increased. The observed trend can be attributed to the catalytic effect and larger surface area of the nano additive. For the same dosage of nano-additive (60 ppm), DiSOME-PG operation with Al2O3 and MWCNT nanoparticles provided increased CD 7.4 % and 4.8 % compared to the same fuel combination with AlO(OH) nano-additive. However, with addition of AlO (OH) in the DiSOME-PG combination resulted in an amplified CD by 5.2 % than diesel-PG operation and lowered by 11.4 % to DiSOME-PG operation.

The addition of AlO(OH) to the DiSOME-PG combination provides not only oxygen but also it provides hydrogen during combustion. Further, the crystalline nature of nanoparticles enhances the combustion. Therefore, oxidation and burning ratesare improved. Also, it is caused by the presence of both oxygen and hydrogen in the AlO(OH) nano-particle leading to increased flame

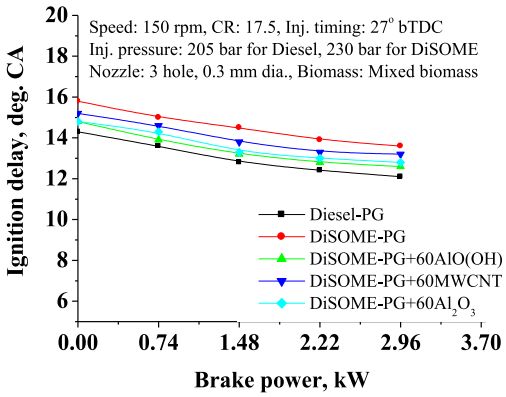

Fig. 23. Effect of different nanoparticles on the variation of ignition delay.

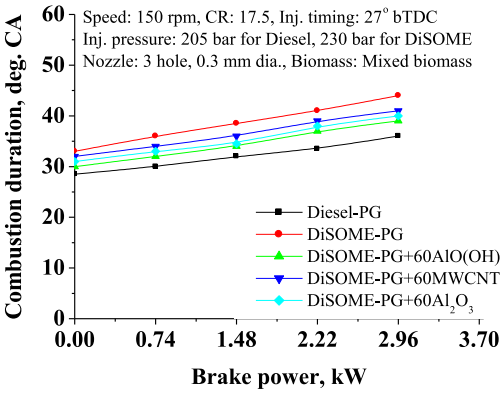

Fig. 24. Effect of different nanoparticles on the variation of combustion duration.

speed and it has low ignition energy resulting in the burning of the fuel combination very fast. In addition, the enhanced character of diffusivity of hydrogen and inbuilt oxygen of AlO(OH) nanoparticle amplifies mixture quality resulting in improved dispersion in the air-PG mixture.

Fig. 25 illustrates the fluctuation in in-cylinder pressure, while Fig. 26 displays the heat release rate (HRR) concerning crank angle for various fuel combinations, both with and without the inclusion of nanoparticles, at 80 % load. Biofuel operation provides always lower performance due to inferior properties [71]. With PG remaining the same, the results demonstrated that, at 80 % load, DiSOME-PG operation produced comparatively reduced HRR and cylinder pressure by 4.6 % and 8.6 %, respectively, in comparison to diesel-based operation. This could be attributed to the low qualities of PG and DiSOME, which result in mixture heterogeneity, decreased flame velocity, and insufficient mixture combustion. Cylinder pressure and HRR were greatly dependent on the quality and quantity of fuel during the rapid combustion phase. In addition, it affects mixture quality during ID, which decides the combustion behavior. Results showed that the addition of NPs improves the combustion of biodiesel-PG mixture due to the greater burning quality of NPs. Further, the DiSOME-PG combination with 60 ppm Al2O3 and MWCNT provided diminished cylinder pressure and HRR by 3.4 % and 4.3 % compared to the same fuel combination with Al(OH) nanoparticle. Similarly, 60 ppm Al2O3 and MWCNT addition resulted in decreased HRR by 8.3 % and 13.4 % respectively compared to the same fuel combination with AlO(OH) nanoparticle. In built oxygen and hydrogen of AlO(OH) provide oxygen and hydrogen during combustion. However, nano-additive to DiSOME provides marginally improved performance [2,24].Further, it may be owing to the absence of oxygen and hydrogen in MWCNT and hydrogen group in Al2O3 nanoparticles. Therefore, improved oxidation rate, amplified mixture homogeneity and increased flame velocity may be the cause for the noticed trend of results. AlO(OH) NPs with hydrogen and oxygen increase oxygen reachability, which enhances the combustible mixture before combustion [63,66,67,72].

When DiSOME-PG dual fuel operation was taken into consideration, it showed a second peak during the diffusion combustion phase in comparison to diesel-PG operation. The primary causes of the trend of results seen in dual fuel operation are caused by oxygen replacement by PG during induction; DiSOME is of inadequate quality; PG contains inert gases; PG reduces air entrainment and mixture quality; PG burns slowly; and the addition of producer gas lowers the cetane number of the fuel combination. Another reason could be that the fuel mixture contains hydrogen, which could lead to a shorter quenching distance. This would enable the flame to go across the combustion chamber more quickly and enhance rapid burning before extinguishing. Also, it could be due to ID reduction and marginally increased cylinder temperature under the nano particles influence. Addition of nanoparticles to DiSOME-PG combination

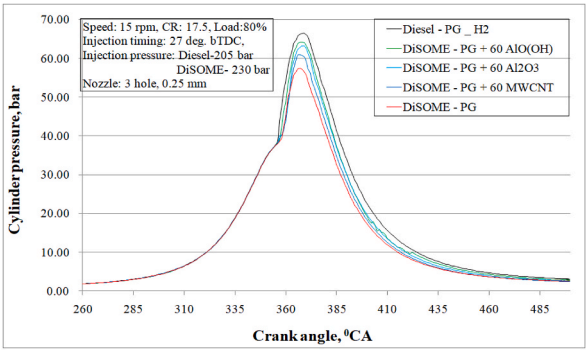

Fig. 25. Cylinder pressure variation concerning crank angle at 80 % load.

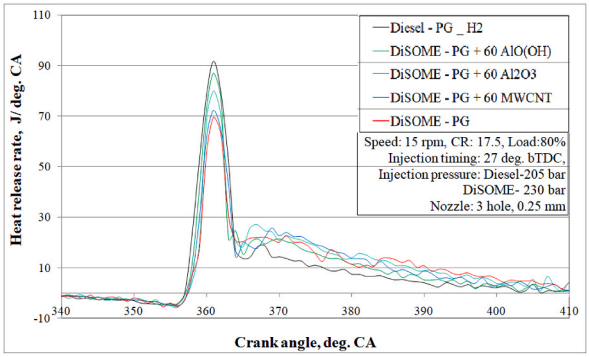

Fig. 26. Heat release rate variation concerning crank angle at 80 % load.

with a large quantity of fuel combination burned during premixed combustion. This enhances the peak cylinder pressure and maximum pressure rise rate. However adequate ignition delay caused by the increased homogeneity of fuel combination and increased cetane number due to the addition of NPs may lead to the increased burning rate and cylinder pressure. The catalytic effect and larger surface area of the nano additives raise the cylinder pressure and HRR. The use of NPs results in improvements in the rate of evaporation, thermal conductivity, and heat release, which enhances the properties of combustion [30]. Results found are within the acceptable range with advanced injection timing and provided smooth combustion and increased combustion temperature and HRR [73,74].

8. Error analysis

In this present work, to reduce errors and obtain a consistent data minimum five set of readings are recorded and averaged out data is used to analyze different engine parameters. Proper methods and procedures are adopted during experimentation. However, random and systematic errors in the data may take place during measurement. Therefore calculated values uncertainty and measured values are recorded. Uncertainties for different parameters such as speed, pressure sensor, BTE, SFC, and smoke, CO, HC, NOx were considered. The overall uncertainty is found to be 2.82.

9. Conclusions

The following are the outcomes of present work drawn from the study:

- ➢ Several previous works of the literature showed that a range variety of nanoparticles with superior properties provide better and emerged encouraging results.
- ➢ Composition and nano-particle blended fuel stability play an important role in improving performance and reduction of emissions. Metal-based and MWCNT nano-additives are good. However, AlO(OH) additives are found to be more successful in amplifying the engine power output with reduced emission levels.
- ➢ The nano-sized additives and stable AlO(OH) particles can provide both oxygen and hydrogen groups during combustion leading to improved engine performance.
- ➢ Investigations showed that DiSOME-PG operation with 20 ppm, 40 ppm, and 60 ppm AlO(OH) and without nano-addition resulted in decreased BTE by 13.6 %, 9.4 %, 2.9 %, and 14.6 % respectively compared to the operation with diesel-based dual fuel operation. But AlO(OH) added biofuel operation provided higher BTE compared to the other nano-additives and neat biodiesel-PG powered dual fuel operation.
- ➢ On average, at 80 % load DiSOME-PG operation showed 26.8 % increased smoke levels compared to diesel-based dual fuel operation. But 60 ppm of AlO(OH) addition to DiSOME-PG operation showed 21.2 % reduced smoke levels compared to neat DiSOME-PG operation. Similarly, HC and CO decreased by 18.5 % and 23.2 % respectively and NOx emissions increased by 32.1 % compared to DiSOME-PG operation.
- ➢ At an optimized nano-particle dosage (60 ppm), MWCNT and Al2O3 nanoparticles-based dual fuel operation provided reduced BTE by 5.45 % and 2.01 % respectively compared to the operation with AlO(OH) nanoparticles at 80 % load. However, DiSOME-PG operation with 60 ppm AlO(OH) nanoparticles resulted in a 5.8 % lowered BTE than diesel-PG operation.
- ➢ DiOSME and producer gas combination at maximum operating conditions, with MWCNT and Al2O3 nanoparticles, resulted in amplified smoke, HC, CO and reduced NOx by 10.8 % and 18.5 %, 13.82 % and 5.8 %, 18.4 % and 8.5 %, and 21.8 % and 12.6 % respectively when compared to AlO(OH) nanoparticles based dual fuel engine for the same fuel combinations at 80 % load.
- ➢ As far as combustion characteristics are concerned, the addition of AlO(OH) nanoparticles to the DiSOME-producer gas combination provided reduced combustion duration, improved cylinder pressure, and heat release rate.
- ➢ DiSOME and producer gas with superior nanoparticles is suitable and its extensive use will deal with energy safety and environmental degradation as well.

➢ Future developments in a biofuel-based engine operation and integrating novel technologies in terms of fuel, hydrogen addition and engine modifications may significantly amplify the engine performance with reduced emission levels.

CRediT authorship contribution statement

K.A. Sateesh: Conceptualization. **V.S. Yaliwal:** Investigation, Data curation. **B.K. Murugande:** Investigation, Conceptualization. **N.R. Banapurmath:** Formal analysis. **P.V. Elumalai:** Methodology. **Dhinesh Balasubramanian:** Writing – review & editing, Writing – original draft, Formal analysis. **Krupakaran Radhakrishnan Lawrence:** Project administration. **Yasser Fouad:** Funding acquisition. **Manzoore Elahi M. Soudagar:** Software. **Huu Cuong Le:** Software. **Thanh Tuan Le:** Validation. **Md Abul Kalam:** Formal analysis. **Chan Choon Kit:** Validation. **Yelamasetti Balram:** Conceptualization.

Declaration of competing interest

The authors declare that they have no known competing financial interests or personal relationships that could have appeared to influence the work reported in this paper.

Acknowledgments

The authors thank the Researchers Supporting Project number (RSPD2025R698), King Saud University, Riyadh, Saudi Arabia, for funding this research. The authors would like to acknowledge the management of DM College of Engineering and Technology, Dharwad and Mepco Schlenk Engineering College, Sivakasi, Tamil Nadu, India for encouraging and supporting the research work.

Data availability

Data will be made available on request.

References

[1] L.T. Popoola, A.O. Agbo, U. Taura, A.S. Yusuff, Y.P. Asmara, O.A. Olagunju, O.M. Chima, Corrosion behavior of aluminum in fossil diesel fuel and biodiesel from chicken eggshell-alumina-catalyzed waste cooking oil, in: Materials and Corrosion, Wiley, 2024, https://doi.org/10.1002/maco.202414510.
[2] M. Srinivasa Rao, R.B. Anand, Performance and emission characteristics improvement studies on a biodiesel fuelled DICI engine using water and AlO(OH) nanoparticles, Appl. Therm. Eng. 98 (2016) 636–645.
[3] V.S. Yaliwal, N.R. Banapurmath, N.M. Gireesh, R.S. Hosmath, T. Donateo, P.G. Tewari, Effect of nozzle and combustion chamber geometry on the performance of a diesel engine operated on dual fuel mode using renewable fuels, Renew. Energy 93 (2016) 483–501.
[4] A.E. Dhole, R.B. Yarasu, D.B. Lata, Investigations on the combustion duration and ignition delay period of a dual fuel diesel engine with hydrogen and producer gas as secondary fuels, Appl. Therm. Eng. 107 (2016) 524–532.
[5] Q. Chen, C. Wang, K. Shao, Yi Liu, X. Chen, Y. Qian, Analyzing the combustion and emissions of a DI diesel engine powered by primary alcohol (methanol, ethanol, n-butanol)/diesel blend with aluminum nano-additives, Fuel 328 (2022) 125222.
[6] C. Srinidhi, Shylesha V. Channapattana, K. Aithal, S. Sarnobath, N.A. Patil, S. Patel, A. Karle, A.A. Mohammed, Relative exergy and energy analysis of DI-CI engine fueled with higher blend of Azadirachta indica biofuel with n-butanol and NiO as fuel additives, Environmental progress and sustainable energy, Am. Inst. Chem. Eng. 43 (3) (2023) 1–8, https://doi.org/10.1002/ep.14336.
[7] Q. Dh, L.M. Geng, H. Chen, Y.Z.H. Bian, C.H.X. Ren, J. Liu, Combustion and performance evaluation of a diesel engine fueled with biodiesel produced from soybean crude oil, Renew. Energy 34 (2009) 2706–2713.
[8] M. Karabektas, The effects of turbocharger on the performance and exhaust emissions of a diesel engine fuelled with biodiesel, Renew. Energy 34 (2009) 989–993.
[9] A. Agarwal, K. Rajamanoharan, Experimental investigations of performance and emissions of Karanja oil and its blends in a single cylinder agricultural diesel engine, Appl. Energy 86 (2009) 106–112.
[10] O. Özener, L. Yüksek, A. Tekin Ergenç, M. Özkan, Effects of soybean biodiesel on a DI diesel engine performance, emission and combustion characteristics, Fuel 115 (2014) 875–883.
[11] N.R. Banapurmath, P.G. Tewari, V.S. Yaliwal, S. Kambalimath, Y.H. Basavarajappa, Combustion characteristics of a 4-stroke CI engine operated on Honge oil, Neem and Rice Bran oils when directly injected and dual fuelled with producer gas induction, Renew. Energy 34 (7) (2009) 1877–1884.
[12] H.V. Srikanth, J. Venkatesh, S. Godiganur, S. Venkateswaran, B. Manne, Bio-based diluents improve cold flow properties of dairy washed milk-scum biodiesel, Renew. Energy 111 (2017) 168–174.
[13] V. Kavitha, V. Geetha, P.J. Jacqueline, Production of biodiesel from dairy waste scum using eggshell waste, Process Saf. Environ. Protect. 125 (2019) 279–287.
[14] P. Sivakumar, K. Anbarasu, S. Renganathan, Bio-diesel production by alkali catalyzed transesterification of dairy waste scum, Fuel 90 (1) (2011) 147, 15.
[15] A. Agarwal, D. Kumar Srivastava, A. Dhar, R. Kumar Maurya, P.C. Shukla, A.P. Singh, Effect of fuel injection timing and pressure on combustion, emissions and performance characteristics of a single cylinder diesel engine, Fuel 111 (2013) 374–383.
[16] V. Karthickeyan, Effect of combustion chamber bowl geometry modification on engine performance, combustion and emission characteristics of biodiesel fuelled diesel engine with its energy and exergy analysis, Energy 176 (2019) 830–852.
[17] Y. Kang, X. Li, H. Shen, Y. Chen, D. Liu, J. Changa, Effects of combustion chamber diameter on the performance and fuel–air mixing of a double swirl combustion system in a diesel engine, Fuel Part A 324 (2022) 124392.
[18] A.T. Doppalapudi, A.K. Azad, M.M.K. Khan, Combustion chamber modifications to improve diesel engine performance and reduce emissions: a review, Renew. Sustain. Energy Rev. 52 (11) (2021) 111683.
[19] S.S. Hoseini, G. Najafi, B. Ghobadian, M.T. Ebadi, R. Mamat, T. Yusaf, Performance and emission characteristics of a CI engine using graphene oxide (GO) nano-particles additives in biodiesel-diesel blends, Renew. Energy 145 (2020) 458–465.
[20] M. Fazal, B. Sazzad, A. Haseeb, Masjuki, Inhibition study of additives towards the corrosion of ferrous metal in palm biodiesel, Energy Convers. Manag. 122 (2016) 290–297.
[21] C.i Srinidhi, S.V. Channapattana, K. Aithal, R. Panchal, S. Dhaneshwar, A. Karle, A. Dharmadikari, A. Gajbhiye, S. Sarnobat, Thermodynamic and Exhaust Emission Studies of CI Engine Powered by Neem Oil Methyl Ester Blends Doped with Nickel Oxide Nano Additives, vol. 43, 2024, https://doi.org/10.1002/ep.14437, 5.

[22] F. Bär, H. Hopf, M. Knorr, O. Schröder, J. Krahl, Effect of hydrazides as fuel additives for biodiesel and biodiesel blends on NOx formation, Fuel 180 (2016) 278–283.
[23] K. Simhadri, P. Srinivasa Rao, M. Paswan, Improving the combustion and emission performance of a diesel engine with TiO2 nanoparticle blended Mahua biodiesel at different injection pressures, Int. J. Thermo Fluid. 21 (2024) 100563.
[24] M.E.M. Soudagar, N.N. Nik-Ghazali, M. Abul Kalam, I.A. Badruddin, N.R. Banapurmath, N. Akram, The effect of nano-additives in diesel-biodiesel fuel blends: a comprehensive review on stability, engine performance and emission characteristics, Energy Convers. Manag. 178 (2018) 146–177.
[25] T. Shaafi, K. Sairam, A. Gopinath, G. Kumaresan, R. Velraj, Effect of dispersion of various nanoadditives on the performance and emission characteristics of a CI engine fuelled with diesel, biodiesel and blends—a review, Renewable Sustainable Energy Rev. 49 (2015) 563–573.
[26] S. Channapattana, S. Campli, A. Madhusudhan, S. Notla, R. Arkerimath, M. Kumar Tripathi, Energy analysis of DI-CI engine with nickel oxide nanoparticle added azadirachta indica biofuel at different static injection timing based on exergy, Energy 267 (2023) 126622, https://doi.org/10.1016/j.energy.2023.126622.
[27] K. Nanthagopal, R.S. Kishna, A.E. Atabani, H. Ala'a-Muhtaseb, K. Gopalakrishnan, B. Ashok, A compressive review on the effects of alcohols and nanoparticles as an oxygenated enhancer in compression ignition engine, Energy Convers. Manag. 203 (2020) 112244.
[28] T. Kegl, A.K. Kralj, B. Kegl, M. Kegl, Nanomaterials as fuel additives in diesel engines: a review of current state, opportunities, and challenges, Prog. Energy Combust. Sci. 83 (2021) 100897.
[29] M. Karagoz, C. Uysal, U. Agbulut, S. Saridemir, Exergetic and exergo-economic analyses of a CI engine fueled with diesel-biodiesel blends containing various metal-oxide nano-particles, Energy 214 (2021) 118830.
[30] M.S. Gad, S. Jayaraj, A comparative study on the effect of nano-additives on the performance and emissions of a diesel engine run on Jatropha biodiesel, Fuel 267 (2020) 117168.
[31] Ü. Ağbulut, M. Karagöz, S. Sarıdemir, A. Öztürk, Impact of various metal-oxide based nanoparticles and biodiesel blends on the combustion, performance, emission, vibration and noise characteristics of a CI engine, Fuel 270 (2020) 117521.
[32] P. Ramesh, S. Vivekanandan, D. Prakash Sivaramakrishnan, Performance optimization of an engine for canola oil blended diesel with Al2O3 nanoparticles through single and multi-objective optimization techniques, Fuel 288 (2021) 119617.
[33] M.E.M. Soudagar, N.N. Nik-Ghazali, M.A. Kalam, I.A. Badruddin, N.R. Banapurmath, M.A. Bin Ali, S. Kamangar, H.M. Cho, N. Akram, An investigation on the influence of aluminium oxide nano-additive and honge oil methyl ester on engine performance, combustion and emission characteristics, Renew. Energy 146 (2020) 2291–2307.
[34] C.i Srinidhi, S.V. Channapattana, K. Aithal, R. Panchal, S. Dhaneshwar, A. Karle, A. Dharmadikari, A. Gajbhiye, S. Sarnobat, Thermodynamic and Exhaust Emission Studies of CI Engine Powered by Neem Oil Methyl Ester Blends Doped with Nickel Oxide Nano Additives, vol. 43, 2024, https://doi.org/10.1002/ep.14437, 5.
[35] Y. Alex, J. Earnest, A. Raghavan, R.G. Roy, C.P. Koshy, Study of engine performance and emission characteristics of diesel engine using cerium oxide nanoparticles blended orange peel oil methyl ester, Energy Nexus 8 (2022) 100150.
[36] M. Sivakumar, N.S. Sundaram, R. Ramesh kumar, M.H. Syed Thasthagir, Effect of aluminium oxide nanoparticles blended pongamia methyl ester on performance, combustion, and emission characteristics of diesel engine, Renew. Energy 116 (2018) 518–526.
[37] M. Ghanbari, L. Mozafari-Vanani, M. Dehghani-Soufi, A. Jahanbakhshi, Effect of alumina nanoparticles as additive with diesel–biodiesel blends on performance and emission characteristic of a six-cylinder diesel engine using response surface methodology (RSM), Energy Convers. Manag. 11 (2021) 100091.
[38] K. Heydari-Maleney, A. Taghizadeh-Alisaraei, B. Ghobadian, A. Abbaszadeh-Mayvan, Analyzing and evaluation of carbon nanotubes additives to diesohol-B2 fuels on performance and emission of diesel engines, Fuel 196 (2017) 110–123.
[39] R.A. Alenezi, A.M.R. Norkhizan, Mamat, G. Erdiwansyah Najafi, M. Mazlan, Investigating the contribution of carbon nanotubes and diesel-biodiesel blends to emission and combustion characteristics of diesel engine, Fuel 285 (2021) 119046.
[40] J. Nagarajan, D. Balasubramanian, Effect of calcium oxide nano fluid additive on diesel engine characteristics fuelled with ternary blend, in: SAE Technical Paper 2021-28-0236, 2021.
[41] S. Pan, J. Wei, C. Tao, G. Lv, Y. Qian, Q. Liu W. Han, Discussion on the combustion, performance and emissions of a dual fuel diesel engine fuelled with methanol-based CeO2 nanofluids, Fuel 302 (2021) 121096.
[42] G. Ramakrishnan, P. Krishnan, S. Rathinam, R. Thiyagu, Y. Devarajan, Role of nano-additive blended biodiesel on emission characteristics of the research diesel engine, Int. J. Green Energy 16 (2019) 435–441.
[43] N. Chacko, T. Jeyaseelan, Comparative evaluation of graphene oxide and graphene nanoplatelets as fuel additives on the combustion and emission characteristics of a diesel engine fuelled with diesel and biodiesel blend, Fuel Process. Technol. 204 (2020) 106406.
[44] S.M.S. Ardebili, A. Taghipoor, H. Solmaz, M. Mostafaei, The effect of nano-iochar on the performance and emissions of a diesel engine fueled with fusel oil-diesel fuel, Fuel 268 (2020) 117356.
[45] P.P. Parikh, A.G. Bhave, D.V. Kapse, Shashikantha, study of thermal and emission performance of small gasifier-dual-fuel engine systems, Biomass 19 (1–2) (1989) 75–97.
[46] N.R. Banapurmath, P.G. Tewari, Comparative performance studies of a 4-stroke CI engine operated on dual fuel mode with producer gas and Honge oil and its methyl ester (HOME) with and without carburettor, Renew. Energy 34 (4) (2009) 1009–1015.
[47] S.S. Halewadimath, V.S. Yaliwal, N.R. Banapurmath, A.M. Sajjan, Influence of hydrogen enriched producer gas (HPG) on the combustion characteristics of a CRDI diesel engine operated on dual-fuel mode using renewable and sustainable fuels, Fuel 270 (2020) 117575, https://doi.org/10.1016/j.fuel.2020.117575.
[48] B.B. Sahoo, N. Sahoo, U.K. Saha, Effect of engine parameters and type of gaseous fuel on the performance of dual-fuel gas diesel engines – a critical review, Renew. Sustain. Energy Rev. 13 (6–7) (2009) 1151–1184.
[49] V.S. Yaliwal, N.R. Banapurmath, V.N. Gaitonde, M.D. Malipatil, Simultaneous optimization of multiple operating engine parameters of a biodiesel-producer gas operated compression ignition (CI) engine coupled with hydrogen using response surface methodology, Renew. Energy 139 (2019) 944–959.
[50] Shashikantha, P.P. Parikh, Spark ignition producer gas engine and dedicated compressed natural gas engine - technology development and experimental performance optimisation, SAE Technical Paper 1999-01-3515 (1999), https://doi.org/10.4271/1999-01-3515.
[51] V.S. Yaliwal, N.R. Banapurmath, N.M. Gireesh, P.G. Tewari, Production and utilization of renewable and sustainable gaseous fuel for power generation applications: a review of literature, Renew. Sustain. Energy Rev. 34 (2014) 608–627.
[52] A.S. Ramadas, S. Jayaraj, C. Muralidharan, Power generation using coir pith and wood derived producer gas in a diesel engine, Fuel Process. Technol. 87 (2006) 849–853.
[53] M. Sharma, R. Kaushal, Performance and exhaust emission analysis of a variable compression ratio (VCR) dual fuel CI engine fuelled with producer gas generated from pistachio shells, Fuel 283 (2021) 118924.
[54] N.L. Panwar, R. Kothari, V.V. Tyagi, Thermo chemical conversion of biomass – eco friendly energy routes, Renew. Sustain. Energy Rev. 16 (4) (2012) 1801–1816.
[55] N.S. Rathore, N.L. Panwar, Y. Vijay Chiplunkar, Design and techno economic evaluation of biomass gasifier for industrial thermal applications, Afr. J. Environ. Sci. Technol. 3 (1) (2008) 6–12.
[56] N.V. Ramalingam Mahalakshmi, Influence of Moringa oleifera biodiesel–diesel–hexanol and biodiesel–diesel–ethanol blends on compression ignition engine performance, combustion and emission characteristics, Royal Soc. Chem. 10 (2020) 4274–4285.
[57] A.P. Carlucci, A. Ficarella, D. Laforgia, L. Strafella, Improvement of dual-fuel biodiesel-producer gas engine performance acting on biodiesel injection parameters and strategy, Fuel 209 (2017) 754–768.
[58] M.M. Roy, E. Tomita, N. Kawahara, Y. Harada, A. Sakane, Performance and emission comparison of a supercharged dual-fuel engine fueled by producer gases with varying hydrogen content, Int. J. Hydrogen Energy 34 (18) (2009) 7811–7822.
[59] N.R. Banapurmath, P.G. Tewari, R.S. Hosmath, Experimental investigations of a four-stroke single cylinder direct injection diesel engine operated on dual fuel mode with producer gas as inducted fuel and Honge oil and its methyl ester (HOME) as injected fuels, Renew. Energy 33 (9) (2008) 2007–2018.

[60] S.K. Nayak, P.C. Mishra, Combustion characteristics, performances, and emissions of a biodiesel-producer gas dual fuel engine with varied combustor geometry, Energy 168 (2019) 585–600.
[61] T.J. Britz, C. Schalkwyk, Y. Hung, Treatment of Dairy Processing Wastewaters, Taylor and Francis Group, LLC, 2006, pp. 1–28.
[62] K.V. Yatish, H.R. Harsha Hebbar, M. Sakar, R. Geetha Balakrishna, A comprehensive review on dairy waste-scum as a potential feedstock for biodiesel production, Process Saf. Environ. Protect. 160 (2022) 921–947.
[63] F.K. Silva, A. Rozineide, A.B. Santa, M.A. Fiori, T. Fernandes de Aquino, C. Soares, M.A. Pignatel Marcon Martins, N. Padoin, H.G. Riella, Synthesis of aluminum hydroxide nanoparticles from the residue of aluminum anodization for application in polymer materials as antiflame agents, J. Mater. Res. Technol. 9 (4) (2020) 8937–8952.
[64] M. Sarnoab, M. Iuliano, Biodiesel production from dairy waste scum by using a efficient nano-biocatalyst, Chem. Eng. Trans. 79 (2020) 191, 186.
[65] E. Khalife, M. Tabatabaei, B. Najafi, M. Mirsalim, A. Gharehghani, P. Mohammadi, M. Aghbashlo, A. Ghaffari, Z. Khounani, T.R. Shojaei, M. Salleh, A novel emulsion fuel containing aqueous nano cerium oxide additive in diesel-biodiesel blends to improve diesel engines performance and reduce exhaust emissions, Part I – experimental analysis, Fuel 207 (2017) 741–750.
[66] K. Yasin, S. Tarkan, Y. Levent, S.D. Ahmet, W. Somchai, Effect of hydrogen–diesel dual-fuel usage on performance, emissions and diesel combustion in diesel engines, Adv. Mech. Eng. 8 (8) (2016) 1–13.
[67] V. Praveen, S. Ashwath Narayanan, G. Hariskousik, K. Balavinayagam, Effect of aluminium oxide hydroxide Nano fluid in castor oil biodiesel fuelled diesel engine, in: 2nd International Conference on Advances in Mechanical Engineering (ICAME 2018), IOP Conf. Series: Materials Science and Engineering, vol. 402, 2018, pp. 1–10.
[68] S. Senthil Kumar, K. Rajan, V. Mohanavel, Manickam Ravichandran, Parvathy Rajendran, Ahmad Rashedi, Abhishek Sharma, Sher Afghan Khan, Asif Afzal, Combustion, performance, and emission behaviors of biodiesel fueled diesel engine with the impact of alumina nanoparticle as an additive, Sustain., MDPI 13 (21) (2021) 12103.
[69] N.H. Papu, P. Lingfa, S.K. Dash, Euglena Sanguinea algal biodiesel and its various diesel blends as diesel engine fuels: a study on the performance and emission characteristics, in: Energy Sources, Part A: Recovery, Utilization, and Environmental Effects, Vol. 46, Informa UK Limited, 2020, pp. 12620–12632. https://doi.org/10.1080/15567036.2020.1798566. Issue 1.
[70] P. Tewari, E. Doijode, N.R. Banapurmath, V.S. Yaliwal, Experimental investigations on a diesel engine fuelled with multiwalled carbon nanotubes blended biodiesel fuels, Int. J. Emerg. Technol. Adva. Eng.(ICERTSD), Special Issue-3 (3) (2013) 72–76.
[71] V.S. Yaliwal, N.R. Banapurmath, Combustion and emission characteristics of a compression ignition engine operated on dual fuel mode using renewable and sustainable fuel combinations, SN Appl. Sci. 3 (2021) 1–24.
[72] S. Pawar, J. Hole, M. Bankar, S. Channapattana, C. Srinidhi, Use of Taguchi method for optimizing engine parameters of Variable Compression Ratio Diesel Engine using Cocklebur seed oil biodiesel blended with Karanja oil biodiesel, Mater. Today: Proc. (2023), https://doi.org/10.1016/j.matpr.2023.08.129.
[73] L. Yu, W. Zi-yu, G. Jian, P. Jun-ru, L. Fu-qiang, Analysis of heat release rate of a diesel engine using Jatropha curcas oil as fuel, in: International Conference on Electric Information and Control Engineering, 2011, pp. 5691–5694, https://doi.org/10.1109/ICEICE.2011.5776900. Wuhan, China.
[74] S.K. Dash, D. Dash, P.K. Das, et al., Investigation on the adjusting compression ratio and injection timing for a DI diesel engine fueled with policy-recommended B20 fuel, Discov Appl Sci 6 (2024) 387. https://doi.org/10.1007/s42452-024-06076-w.